

# Congestion Reduction via Personalized Incentives

Ali Ghafelebashi\*, Meisam Razaviyayn, and Maged Dessouky

Daniel J. Epstein Department of Industrial & Systems Engineering, University of Southern California,  
3715 McClintock Avenue, Los Angeles, CA 90089, United States

## Abstract

With rapid population growth and urban development, traffic congestion has become an inescapable issue, especially in large cities. Many congestion reduction strategies have been proposed in the past, ranging from roadway extension to transportation demand management. In particular, congestion pricing schemes have been used as negative reinforcements for traffic control. In this paper, we study an alternative approach of offering positive incentives to drivers to take different routes. More specifically, we propose an algorithm to reduce traffic congestion and improve routing efficiency via offering (personalized) incentives to drivers. We propose to exploit the wide accessibility of smart devices to communicate with drivers and develop an incentive offering mechanism using individuals' preferences and aggregate traffic information. The incentives are offered after solving a large-scale optimization problem in order to minimize the total travel time (or minimize any cost function of the network such as total carbon emission). Since this massive-size optimization problem needs to be solved continually in the network, we developed a distributed computational approach. The proposed distributed algorithm is guaranteed to converge under a mild set of assumptions that are verified with real data. We evaluated the performance of our algorithm using traffic data from the Los Angeles area. Our experiments show congestion reduction of up to 5% in arterial roads and highways.

## Index Terms

Congestion Reduction, Personalized Incentives, Travel Demand Management, Behavior Change.

## I. INTRODUCTION

Today, traffic congestion is one of the most prevalent issues in large metropolitan areas, resulting in lower quality of life for residents, economic losses, worsen air quality, and adversely affecting health conditions [1–6]. In this paper, we study the problem of offering incentives to drivers to affect their behavior and reduce traffic congestion. Our methodology is closely related to the pricing mechanisms in the literature. Road pricing policies, such as assigning a fee or tax for driving on a highway/road, have been widely studied in theory and practice [7–11]. Pricing strategies may depend on different factors such as time of the travel [12], distance [13], or vehicle characteristics [14]. While pricing is a promising approach from a market point of view, issues such as equity

\*Corresponding author at: 3650 McClintock Ave., Los Angeles, CA 90089, United States.

*Email addresses:* ghafeleb@usc.edu (Ali Ghafelebashi), razaviya@usc.edu (Meisam Razaviyayn), maged@usc.edu (Maged Dessouky).

barriers complicate the implementation of congestion pricing/taxation schemes [15–20]. In addition, complexities and uncertainties in designing pricing mechanisms have prevented policymakers from implementing advanced congestion pricing schemes [21]. Tradable credits (TCs) or tradable mobility permits (TPMs) are other token-based pricing mechanisms [22–27]. The theoretical advantages of such tradable credits have been shown in [28–31]. While such cap-and-trade programs have been implemented in some economic sectors, such as airport slot allocation [32], it has not been implemented for individual-level personal travel and daily commute [33] due to the design complexities of such token markets [34]. In addition, they do not consider the personalized preference of different drivers.

Lately, researchers have paid more attention to positive incentive policies. Based on the psychological theory of reactance, rewarding desirable behavior could work better than penalizing undesirable behavior [35]. Moreover, rewarding is a more popular policy than a taxation approach [36]. While the effectiveness of rewarding in changing the individual's behavior has been shown in [37] and [38], there are a limited number of studies on the effectiveness of rewarding policies in the transportation area. Among these studies, the INSTANT project [39], the CAPRI project [40], and a series of studies in the Netherlands [41–44] have shown the effectiveness of a rewarding policy in congestion reduction in limited settings. However, none of these methodologies can consider the personalized preferences of individual drivers. Another form of reward was recently studied in [34] where tokens were offered for different travel choices such as route, travel modes, and ride-sharing. The proposed model learns individuals' decisions and adapts to their preferences based on their travel history. While these policies were successful in short-term experiments, they did not necessarily result in permanent changes in the travelers' behavior [45]. More recently, [46] and [47] provide incentives to (or charge) volunteer truck drivers to improve the overall traffic condition in a budget balanced mechanism. [48] considers VOT (Value of Time) in the mechanism to make it personalized. There have been different choices used as the incentive in transportation studies such as free bus tickets [49, 50], early bird tickets [51], free WiFi and discounted fares [52], money [15], and tokens [34].

The preferences of the drivers in selecting different routes can be considered in the incentive offering platform. Mohan et al studied different factors impacting drivers' decision for routing in [53]. They partitioned these factors into two categories of static factors and dynamic factors. The static factors, which are fixed for different people, include the number of available transportation options and the distance of nearby transit. On the other hand, the dynamic factors include weather and travel purpose, which changes from one person to another. They identified these factors by performing interviews and surveys and concluded that personalizing the incentives can be advantageous. Also, the driver's preferences can be learned through interaction with the individual [34, 54]. The goal of offering personalized incentives is to closely tie the offer to the individual's preferences, thus maximizing the probability of changing the drivers' behaviors [54].

In this paper, we study the problem of offering personalized incentives to minimize a global cost function in the network. Although previous studies (e.g. [41]) consider static rewards for static options like teleworking, biking, and walking, our model assigns different rewards for different alternative routes for different drivers based on the traffic condition and personalization factors. Consequently, we have more freedom in offering incentives, and our methodology results in an optimization problem with a larger number of decision variables. The implementation of

our proposed model could be through a smartphone app where the traffic data can be used to offer incentives to drivers. In addition, smartphones will help the central planner to distribute the computational load for finding the optimal incentive offering strategy. The rest of this paper is organized as follows: At the beginning of Section II, we present our model. Then, in subsection II-C, we propose a distributed algorithm to solve our optimization problem efficiently. Results of our numerical experiments are presented in Section III using data from the Los Angeles area. Finally, we conclude in section IV. The details of our methodology and experiments are provided in the appendix.

## II. INCENTIVE OFFERING MECHANISMS

Let us model the structure of the traffic network with a directed graph  $\mathcal{G} = (\mathcal{V}, \mathcal{E})$ . Here  $\mathcal{V}$  is the collection of all major intersections and ramps, which form the set of nodes in the graph. We use the set of edges  $\mathcal{E}$  to capture the connectivity of the nodes in the graph. Two different nodes are adjacent in the graph if it is possible to directly go from one to another without passing over any other node. The direction of an edge between two nodes is based on the direction of the road from which we can go from one point to another. We also use the notation  $|\mathcal{E}|$  to denote the total number of road segments/edges in our network (i.e. the cardinality of the set  $\mathcal{E}$ ). A route is a collection of adjacent edges that starts from one node and ends in another. We use the one-hot encoding scheme to denote the routes. In other words, a given route is represented by a vector  $\mathbf{r} \in \{0, 1\}^{|\mathcal{E}|}$ . Here, the  $k$ -th entry of vector  $\mathbf{r}$  is one if the  $k$ -th edge is a part of route  $\mathbf{r}$  and it is zero, otherwise.

Let  $\mathbf{T} = \{1, \dots, T\}$  denote the time horizon of interest assuming the system is currently at time  $t = 1$ . For any  $t \in \mathbf{T}$ , we use the random vector  $\mathbf{v}_t \in \mathbb{R}^{|\mathcal{E}|}$  to represent the traffic volume on the different road segments at time  $t$ . The  $k$ -th entry of  $\mathbf{v}_t$  shows the total number of vehicles of road segment  $k$  at time  $t$ . Notice that the offered incentives can change the drivers' behavior who are using the platform in the future and thus affecting the vector  $\mathbf{v}_t$ .

We use  $\mathcal{N}$  to denote the set of drivers that we can influence their behavior through offering incentives. For any driver  $n \in \mathcal{N}$ , let  $\mathcal{R}_n \subseteq \{0, 1\}^{|\mathcal{E}|}$  denote the set of possible route options for going from its origin to its destination. Let  $\mathcal{I}_n$  be the set of possible incentives we can offer to driver  $n \in \mathcal{N}$ . We also use the binary variable  $s_i^{\mathbf{r}, n} \in \{0, 1\}$  to represent the offered incentives. For any driver  $n \in \mathcal{N}$  and incentive  $i \in \mathcal{I}_n$ , the variable  $s_i^{\mathbf{r}, n} = 1$  if incentive  $i$  is offered to driver  $n$  to take route  $\mathbf{r}$ ; and  $s_i^{\mathbf{r}, n} = 0$  otherwise. We assume that we incentivize each driver with only one offer, i.e.,  $\sum_{\mathbf{r} \in \mathcal{R}_n} \sum_{i \in \mathcal{I}_n} s_i^{\mathbf{r}, n} = 1$ . Given any incentive offered to the drivers, we model the decision of the drivers stochastically. In particular, we assume after offering incentives, each driver  $n$  chooses route  $\mathbf{r}$  with a certain probability which depends on the amount of incentive, the route, and the driver's preferences, as described below.

The route preferences of the drivers depend on different factors such as route travel time, gender, age, and particularly the (monetary) incentive provided to the drivers in our context. Such dependence can be learned using standard machine learning approaches in the presence of data [55]. In this project, we rely on the model developed in [55] for our preference modeling. We simplify their model by not including the less predictive features and only considering two major features: the value of incentive and travel time. In particular, we assume that, given

incentive  $i \in \mathcal{I}_n$  to driver  $n$ , the driver chooses route  $\mathbf{r}$  with probability

$$p_i^{\mathbf{r},n} = P(\widehat{T}_{\mathbf{r}}, i), \quad (1)$$

where  $\widehat{T}_{\mathbf{r}}$  is the estimate of the travel time for route  $\mathbf{r}$  provided by the incentive offering platform. Notice that when drivers make their routing decisions, they do not know the exact travel time  $T_{\mathbf{r}}$  for route  $\mathbf{r}$ , but instead, they rely on the estimate  $\widehat{T}_{\mathbf{r}}$  provided by the system. Here, we make an implicit assumption that the drivers do not consider their own judgment about the travel time in their decision. However, if such individual biases for drivers exist, the system can learn them over time using standard preference learning techniques. Modeling the drivers' behavior in a probabilistic fashion has its own benefits. The decision of a driver for a given incentive amount depends on many factors such as age, gender, and income as also studied in [55]. It is even likely that the driver's decision may depend on the driver's "state of mind" at the time that the incentive is offered. Thus, the features that influence the driver's decision are not completely known to the central planner. In such a setting, probabilistic models can be a better fit for modeling the system. For this reason, in the general area of "recommendation systems" in machine learning and statistics, probabilistic models have been widely used to model the behavior of individual users (drivers in our setting) [56]. In addition, we do not assume any traffic control by modeling the probability of drivers' acceptance. Traffic control might be more effective but it needs an authority with the power of changing traffic which is not required in our framework. In our model, drivers can disregard the offers at any time but the offers change the probability of accepting drivers' routing choices.

In the next subsections, we present our model and formulation in more detail. For the convenience of the reader, the list of notations defined here and later in the manuscript is presented in Appendix A. We present our framework under two different scenarios: First, for simplicity of presenting the ideas, we study the case where it is possible to bring traffic flow below the network capacity. Then, we study the high demand scenario where there is no feasible strategy to bring the demand below the network capacity.

#### A. Scenario I: Operating Below Network Capacity

Let us first for simplicity assume that there exists a solution that all road segments operate below capacity. Hence, for that solution, we can assume that the travel time will be based on the free flow traffic. As this section shows, this assumption will result in a mixed integer linear programming optimization which can be solved efficiently using standard solvers.

Given (1), the expected value of the volume vector  $\mathbf{v}_t$  can be computed as:

$$\mathbb{E}[\mathbf{v}_t] = \sum_{n \in \mathcal{N}} \sum_{i \in \mathcal{I}_n} \sum_{\mathbf{r} \in \mathcal{R}_n} s_i^{\mathbf{r},n} p_i^{\mathbf{r},n} \boldsymbol{\beta}_{\mathbf{r},t} \quad (2)$$

where the vector  $\boldsymbol{\beta}_{\mathbf{r},t} \in \mathbb{R}^{|\mathcal{E}|}$  shows the probability of being at different links of the network at time  $t \in \mathbf{T}$ , conditioned on the fact that driver  $n$  is on route  $\mathbf{r}$ . For more details about the vector  $\boldsymbol{\beta}_{\mathbf{r},t}$ , please refer to [57].

In order to minimize the drivers' total travel time while keeping the volume below the road segment capacity

vector  $\mathbf{v}_0$ , we need to solve the following optimization problem

$$\begin{aligned}
& \min_{\{s_i^{r,n}\}} \sum_{t \in \mathbf{T}} \sum_{n \in \mathcal{N}} \sum_{r \in \mathcal{R}_n} \sum_{i \in \mathcal{I}_n} s_i^{r,n} p_i^{r,n} \beta_{r,t}^\top \boldsymbol{\omega} \\
& \text{s.t.} \quad \sum_{n \in \mathcal{N}} \sum_{i \in \mathcal{I}_n} \sum_{r \in \mathcal{R}_n} s_i^{r,n} p_i^{r,n} \beta_{r,t} \leq \mathbf{v}_0, \quad \forall t \in \mathbf{T} \\
& \quad \sum_{n \in \mathcal{N}} \sum_{i \in \mathcal{I}_n} \sum_{r \in \mathcal{R}_n} s_i^{r,n} \eta_i \leq \Omega \\
& \quad \sum_{r \in \mathcal{R}_n} \sum_{i \in \mathcal{I}_n} s_i^{r,n} = 1 \quad \forall n \in \mathcal{N} \\
& \quad s_i^{r,n} \in \{0, 1\} \quad \forall n \in \mathcal{N}, \forall i \in \mathcal{I}_n, \forall r \in \mathcal{R}_n
\end{aligned} \tag{3}$$

where  $\boldsymbol{\omega} \in \mathbb{R}^{|\mathcal{E}|}$  is the vector of free flow travel time of the links,  $\Omega$  is the total available budget, and  $\eta_i$  is the cost of offering incentive  $i$ . To keep this optimization problem tractable, we rely on the assumption of a large number of vehicles in each road segment and approximate the random quantity  $\mathbf{v}_t$  with its average  $\mathbb{E}[\mathbf{v}_t]$  provided in equation (2). Notice that the objective function is equal to

$$\min_{\{s_i^{r,n}\}} \sum_{n \in \mathcal{N}} \sum_{r \in \mathcal{R}_n} \sum_{i \in \mathcal{I}_n} s_i^{r,n} p_i^{r,n} \sum_{t \in \mathbf{T}} \beta_{r,t}^\top \boldsymbol{\omega}$$

in which  $\sum_{t \in \mathbf{T}} \beta_{r,t}^\top \boldsymbol{\omega}$  is the expected travel time of driver  $n$  driving on route  $r$ .

Problem (3) is a mixed integer linear program that can be solved via standard solvers such as Gurobi, AMPL, GAMS, and CPLEX. We use Gurobi in our experiments because of its powerful LP solver.

### B. Scenario II: Operating Above Network Capacity

In this subsection, we assume that the demand is elevated; thus, there is no incentive offering strategy that can bring the traffic flow below the network capacity. In such a scenario, we still can “improve” the congestion by incentivizing individual drivers. Our goal is to optimize a disutility of the system as a criterion to compare the traffic condition after incentivizing. To make the formulation more specific, we use total travel time as the disutility function. It is worth noting that while we use this disutility, following our steps, one can use any other disutility function such as carbon emissions or energy consumption.

To compute the total travel time of the system, we sum the travel time of the drivers of all the links over all time periods:

$$F_{tt}(\hat{\mathbf{v}}) = \sum_{\ell=1}^{|\mathcal{E}|} \sum_{t=1}^{|\mathbf{T}|} \hat{v}_{\ell,t} \delta_{\ell,t}(\hat{v}_{\ell,t}) \tag{4}$$

where  $\delta_{\ell,t}$  is the travel time of link  $\ell$  at time  $t$  (which itself is a function of the volume). Here,  $\hat{\mathbf{v}}$  is the vector of volume of links in which  $\hat{v}_{\ell,t}$  is the  $(|\mathcal{E}| \times t + \ell)^{th}$  element of vector  $\hat{\mathbf{v}}$  representing the volume of the  $\ell^{th}$  link at time  $t$ .

To understand the impact of our offered incentives, we estimate the drivers’ decision based on the provided incentives, which in turn results in estimating the volume of the links in the horizon of interest. Given these estimated volume values, we estimate the travel time in the links as described below.

*Travel time value  $\delta$* : There are different functions that capture the relation between travel time and volume. For example, the link congestion function developed by the Bureau of Public Roads (BPR) [58] defines a nonlinear relation between the volume and travel time of the road segments:

$$f_{\text{BPR}}(v) = t_0 \left( 1 + 0.15 \left( \frac{v}{w} \right)^4 \right)$$

where  $f_{\text{BPR}}(v)$  is the travel time of the drivers on the link given the assigned traffic volume  $v$ ; the parameter  $t_0$  is the free flow travel time of the link;  $v$  is the assigned traffic volume of the link; and  $w$  is the practical capacity of the link. We learn  $t_0$  and  $w$  using historical traffic data. Although we use the BPR function in our presented model, our methodology provides a modular framework in which we can replace the BPR function with any other appropriate function. In order to estimate the total travel time of the system, we need to estimate the volume vector  $\hat{v}$ , which we discuss next.

*Volume vector  $\hat{v}$* : To compute the volume vector, we need to know the routing decision of the drivers to be able to (approximately) estimate their location at different times. Clearly, the drivers' decision is a function of the offered incentives. In other words, the location of a driver is dependent on the incentive that we assign to them because the likelihood of various decisions changes with different incentives. Let us first explain our notations for the offered incentives: For each driver, we have a one-hot encoded vector describing which route has been incentivized and how much reward has been assigned to it. Thus, for each driver we have a binary vector  $\mathbf{s}_n \in \{0, 1\}^{|\mathcal{R}| \cdot |\mathcal{I}|}$  in which only one element has a value of one and it corresponds to the route and the incentive amount that we offer. As we need one vector for each driver, we can aggregate all our incentivization strategies in a matrix  $\mathbf{S} \in \{0, 1\}^{(|\mathcal{R}| \cdot |\mathcal{I}|) \times |\mathcal{N}|}$ . Naturally, routes that are not relevant to that OD pair of a driver will get a value of zero in the corresponding incentive vector (since we cannot offer those routes to the driver).

To understand the drivers' responses to our offered incentives, we need to estimate the probability of acceptance of incentivized routes under different incentives including zero incentive (i.e, no incentive). To model this probability, we use the utility function developed in [55] and compute the probability of acceptance of each offered incentive (by using a Softmax function on top of the utility). While the model in [55] takes many parameters (such as gender, age, and education of the driver) as input, in our model and numerical experiments we only consider static parameters of the travel time and the reward value to generate the probability of acceptance of a given incentive/reward. However, our framework is modular and we can use any prediction model that can estimate drivers' behavior given an incentive amount. We can use any personalized routing model that can learn drivers' behavior such as a neural network. Let  $\mathbf{P} \in [0, 1]^{|\mathcal{R}| \times (|\mathcal{R}| \cdot |\mathcal{I}|)}$  be a matrix encoding the information of probability of picking different routes given the offered (route, incentive) pairs. Thus, the vector  $\mathbf{PS1} \in \mathbb{R}^{|\mathcal{R}| \times 1}$  shows the expected number of vehicles in each route.

Given the number of vehicles in each route, the location of each driver for the next time horizon can be modeled in a probabilistic fashion. For this purpose, we rely on the model developed in [57] where a specific matrix  $\mathbf{R} \in [0, 1]^{(|\mathcal{E}| \cdot |\mathbf{T}|) \times |\mathcal{R}|}$  is proposed to estimate the probability of the presence of a driver in a given road segment at a specific time in the future (assuming that the driver is picking a specific route). We can compute matrix  $\mathbf{R}$

by running a simulation model if we have enough computation power. In our experiments in subsection III-A, we rely on the historical data in computing matrix  $\mathbf{R}$ . Similar to other performative prediction problems [59], an inconsistency may appear between the estimated value and the actual output (as the estimation impacts the outcome). To resolve this issue, we first used the historical travel time to compute matrix  $\mathbf{R}$  in our experiments. Then, we used the estimated  $\mathbf{R}$  to form the objective function. This approach can be viewed as an ‘‘approximation’’ of the actual utility function when we want to compute the incentives. This approximation is only used in computing incentives, and our evaluation of the system’s performance is based on the actual travel times because after the drivers make their decision, computing the actual travel time is possible, and such an inconsistency no longer exists. Thus, the vector

$$\hat{\mathbf{v}} = \mathbf{RPS1} \in \mathbb{R}^{(|\mathcal{E}| \cdot |\mathbf{T}|) \times 1}$$

represents the expected number of vehicles in all the links at each time slot. Substituting the expression of  $\hat{\mathbf{v}}$  in (4), we get

$$\begin{aligned} F_{tt}(\hat{\mathbf{v}}) &= \sum_{\ell=1}^{|\mathcal{E}|} \sum_{t=1}^{|\mathbf{T}|} (\mathbf{AS1})_{\ell,t} \delta((\mathbf{AS1})_{\ell,t}) \\ &= \sum_{\ell=1}^{|\mathcal{E}|} \sum_{t=1}^{|\mathbf{T}|} (\mathbf{a}_{\ell,t} \mathbf{S1}) \delta(\mathbf{a}_{\ell,t} \mathbf{S1}) \end{aligned} \quad (5)$$

where  $\mathbf{a}_{\ell,t}$  is the row of matrix  $\mathbf{A} = \mathbf{RP}$  which corresponds to link  $\ell$  at time  $t$ . Thus in order to minimize the total travel time in the system by providing incentives to drivers, we need to solve the following optimization problem:

$$\begin{aligned} \min_{\mathbf{S}} \quad & \sum_{\ell=1}^{|\mathcal{E}|} \sum_{t=1}^{|\mathbf{T}|} (\mathbf{a}_{\ell,t} \mathbf{S1}) \delta(\mathbf{a}_{\ell,t} \mathbf{S1}) \\ \text{s.t.} \quad & \mathbf{S}^\top \mathbf{1} = \mathbf{1}, \quad \mathbf{c}^\top \mathbf{S1} \leq \Omega \\ & \mathbf{DS1} = \mathbf{q}, \quad \mathbf{S} \in \{0, 1\}^{(|\mathcal{R}| \cdot |\mathcal{I}|) \times |\mathcal{N}|} \end{aligned} \quad (6)$$

where  $\mathbf{c} \in \mathbb{R}_+^{|\mathcal{R}| \cdot |\mathcal{I}|}$  is the vector of cost of incentives assigned to each route,  $\mathbf{D} \in \{0, 1\}^{K \times (|\mathcal{R}| \cdot |\mathcal{I}|)}$  is the matrix of incentive assignment to the OD pairs, and  $\mathbf{q} \in \mathbb{R}^{K \times |\mathcal{I}|}$  is the vector of the number of drivers for each OD pair. Here,  $K$  is the number of OD pairs. We explain the constraints in more detail below:

**Constraint 1** ( $\mathbf{S}^\top \mathbf{1} = \mathbf{1}$ ): This constraint simply states that we only assign one incentive to each driver.

**Constraint 2** ( $\mathbf{c}^\top \mathbf{S1} \leq \Omega$ ): This is our budget constraint. The vector  $\mathbf{c} \in \mathbb{R}^{|\mathcal{R}| \cdot |\mathcal{I}|}$  represents the cost of the different rewards assigned to each driver.  $\Omega$  is the total budget.

**Constraint 3** ( $\mathbf{DS1} = \mathbf{q}$ ): This constraint makes sure that we offer the correct number of rewards for the routes between OD pairs. Recall that  $\mathbf{S1}$  represents the (expected) number of drivers that have been offered different routes given different rewards. We use matrix  $\mathbf{D}$  to sum the number of drivers that received different reward offers for routes between the same OD pair.  $\mathbf{q}$  is the vector of the actual number of drivers that are traveling between OD pairs and  $\mathbf{DS1}$  must be equal to  $\mathbf{q}$ .

**Constraint 4** ( $\mathbf{S} \in \{0, 1\}^{(|\mathcal{R}||\mathcal{I}) \times |\mathcal{N}|}$ ): This constraint imposes binary structure on our decision parameters. In other words, 0 is not choosing an incentive and 1 is selecting the incentive.

To illustrate our model and the above constraints, we provide an example in Appendix E.

### C. Algorithm for Offering Incentives and A Distributed Implementation

The optimization problem (6) is of large size while it needs to be solved in almost real time (or hourly if the drivers send their travel information to the central planner every hour before their trip) in the network. However, due to the existence of binary variable  $\mathbf{S}$ , solving this problem efficiently is difficult\*. In order to develop an efficient “approximate” solver for (6), we first relax the binary constraint in (6) and replace it with the relaxed convex constraint  $\mathbf{S} \in [0, 1]^{(|\mathcal{R}||\mathcal{I}) \times |\mathcal{N}|}$ , leading to the relaxed formulation

$$\begin{aligned} \min_{\mathbf{S}} \quad & \sum_{\ell=1}^{|\mathcal{E}|} \sum_{t=1}^{|\mathcal{T}|} (\mathbf{a}_{\ell,t} \mathbf{S} \mathbf{1}) \delta(\mathbf{a}_{\ell,t} \mathbf{S} \mathbf{1}) \\ \text{s.t.} \quad & \mathbf{S}^T \mathbf{1} = \mathbf{1}, \quad \mathbf{c}^T \mathbf{S} \mathbf{1} \leq \Omega \\ & \mathbf{D} \mathbf{S} \mathbf{1} = \mathbf{q}, \quad \mathbf{S} \in [0, 1]^{(|\mathcal{R}||\mathcal{I}) \times |\mathcal{N}|}. \end{aligned} \tag{7}$$

The constraints in the above optimization problem are convex. By substituting  $\mathbf{a}_{\ell,t} \mathbf{S} \mathbf{1}$  by  $\gamma_{\ell,t}$ , the objective function becomes a summation of monomial functions with positive coefficients. Moreover,  $\gamma_{\ell,t}$  is an affine mapping of the optimization variable  $\mathbf{S}$ . Since our domain is the nonnegative orthant and monomials are convex in this domain, the objective function is convex. This convexity will allow us to explore the use of standard solvers such as CVX [60]. However, these solvers rely on methods such as interior point methods [61] which requires  $O(n^3)$  number of iterations with  $n$  being the number of variables. This heavy computational complexity prevents us from applying standard solvers for realistic size problems. In our context, each driver is equipped with a smartphone and; thus, we can distribute the computational burden of solving (7) among the drivers. In what follows, we propose a simple reformulation of the problem leading to a distributed algorithm for solving (7). To present our algorithm, let us start by reformulating (7) as

$$\begin{aligned} \min_{\gamma, \mathbf{u}, \mathbf{S}, \mathbf{W}, \mathbf{H}, \mathbf{z}, \beta} \quad & \sum_{\ell=1}^{|\mathcal{E}|} \sum_{t=1}^{|\mathcal{T}|} \gamma_{\ell,t} \delta(\gamma_{\ell,t}) \\ & - \frac{\tilde{\lambda}}{2} \sum_{r=1}^{|\mathcal{R}|} \sum_{i=1}^{|\mathcal{I}|} \sum_{n=1}^{|\mathcal{N}|} \mathbf{H}_{r,i,n} (\mathbf{H}_{r,i,n} - 1) \\ \text{s.t.} \quad & \mathbf{S} \mathbf{1} = \mathbf{u}, \quad \mathbf{W}^T \mathbf{1} = \mathbf{1} \\ & \mathbf{D} \mathbf{u} = \mathbf{q}, \quad \mathbf{A} \mathbf{u} = \gamma \\ & \mathbf{H} = \mathbf{S}, \quad \mathbf{W} = \mathbf{S} \\ & \mathbf{c}^T \mathbf{u} + \beta = \Omega, \quad \beta \geq 0 \\ & \mathbf{H} \in [0, 1]^{(|\mathcal{R}| \cdot |\mathcal{I}|) \times |\mathcal{N}|}. \end{aligned} \tag{8}$$

\*We conjecture that problem (6) is NP-hard to solve since it is a special instance of polynomial optimization with discrete variables and there does not appear to be any special structure in function  $f$  to reduce its complexity.

As we discuss in Appendix A, this formulation is amenable to the ADMM method [62–67], which has a natural distributed implementation. Our ADMM formulation (8) shows that this computation burden can be distributed among drivers’ cell phones. This distributed optimization/federated learning framework can have other standard advantages of federated learning/distributed systems [68, 69]. For example, when proper privacy preserving mechanisms (such as differential privacy [70]) are utilized, we can guarantee the privacy of drivers since they can participate in the optimization procedure without completely sharing their data and through a private communication mechanism (see, e.g., [69, 71–73]). The steps of this algorithm are summarized in Algorithm 1 and the details of the derivation of its steps are provided in Appendix A.

It is worth mentioning that other standard approaches such as projected gradient descent is not easily applicable to problem (8) due to the complexity of the projection operator to our constraint set. However, ADMM will decompose this projection across multiple variables with each projection being easy to compute. In addition to projection, computation of the *linear minimization oracle* is also expensive, which eliminates the possibility of utilizing other methods such as the conditional gradient (Frank-Wolfe) method. These are the reasons (in addition to the possibility of distributed implementation) behind choosing ADMM.

---

**Algorithm 1** Distributed Incentivization via ADMM

---

- 1: **Input:** Initial values:  $\gamma^0, \mathbf{S}^0, \mathbf{H}^0, \mathbf{W}^0, \mathbf{u}^0, \beta^0, \boldsymbol{\lambda}_1^0 \in \mathbb{R}^{|\mathcal{R}| \cdot |\mathcal{I}| \times 1}, \boldsymbol{\lambda}_2^0 \in \mathbb{R}^{|\mathcal{N}| \times 1}, \boldsymbol{\lambda}_3^0 \in \mathbb{R}^{K \times 1}, \boldsymbol{\lambda}_4^0 \in \mathbb{R}^{|\mathcal{E}| \cdot \mathbf{T} \times 1}, \boldsymbol{\Lambda}_5^0 \in \mathbb{R}^{|\mathcal{R}| \cdot |\mathcal{I}| \times |\mathcal{N}|}, \lambda_6^0 \in \mathbb{R}, \boldsymbol{\Lambda}_7^0 \in \mathbb{R}^{|\mathcal{R}| \cdot |\mathcal{I}| \times |\mathcal{N}|}$ , Dual update step:  $\rho$ , Number of iterations:  $\tilde{T}$ .
  - 2: **for**  $t = 0, 1, \dots, \tilde{T}$  **do**
  - 3:    $\mathbf{u}^{t+1} = (\rho \mathbf{I} + \rho \mathbf{D}^\top \mathbf{D} + \rho \mathbf{A}^\top \mathbf{A} + \rho \mathbf{c} \mathbf{c}^\top)^{-1} (\boldsymbol{\lambda}_1^t + \rho \mathbf{S}^t \mathbf{1} - \mathbf{D}^\top \boldsymbol{\lambda}_3^t + \rho \mathbf{D}^\top \mathbf{q} - \mathbf{A}^\top \boldsymbol{\lambda}_4^t + \rho \mathbf{A}^\top \boldsymbol{\gamma}^t - \mathbf{c} (\lambda_6^t + \beta^t - \Omega))$
  - 4:    $\mathbf{W}^{t+1} = (\rho \mathbf{1} \mathbf{1}^\top + \rho \mathbf{I})^{-1} (\rho \mathbf{1} \mathbf{1}^\top + \rho \mathbf{S}^t - \boldsymbol{\Lambda}_7^t - \mathbf{1} \boldsymbol{\lambda}_2^{t\top})$
  - 5:    $\mathbf{H}^{t+1} = \mathbb{1}(\rho > \tilde{\lambda}) \Pi \left( \left( \frac{1}{\rho - \tilde{\lambda}} \right) (\rho \mathbf{S}^t - \boldsymbol{\Lambda}_5^t - \frac{\tilde{\lambda}}{2}) \right)_{[0,1]} + \mathbb{1}(\rho < \tilde{\lambda}) \Pi \left( \left( \frac{1}{\rho - \tilde{\lambda}} \right) (\rho \mathbf{S}^t - \boldsymbol{\Lambda}_5^t - \frac{\tilde{\lambda}}{2}) \right)_{\{0,1\}}$
  - 6:    $\mathbf{S}^{t+1} = (\rho \mathbf{u}^{t+1} \mathbf{1}^\top + \boldsymbol{\Lambda}_5^t + \rho \mathbf{H}^{t+1} + \boldsymbol{\Lambda}_7^t + \rho \mathbf{W}^{t+1} - \boldsymbol{\lambda}_1^t \mathbf{1}^\top) (\rho \mathbf{1} \mathbf{1}^\top + 2\rho \mathbf{I})^{-1}$
  - 7:   **for**  $\ell = 0, 1, \dots, |\mathcal{E}|$  **do**
  - 8:     **for**  $\hat{t} = 1, \dots, |\mathbf{T}|$  **do**
  - 9:        $\gamma_{\ell, \hat{t}}^{t+1} = \underset{\gamma_{\ell, \hat{t}}}{\operatorname{argmin}} \gamma_{\ell, \hat{t}} \delta(\gamma_{\ell, \hat{t}}) + \boldsymbol{\lambda}_{4, (\ell, \hat{t})}^t (\mathbf{a}_{\ell, \hat{t}} \mathbf{u}^t - \gamma_{\ell, \hat{t}}) + \frac{\rho}{2} (\mathbf{a}_{\ell, \hat{t}} \mathbf{u}^t - \gamma_{\ell, \hat{t}})^2$
  - 10:     **end for**
  - 11:   **end for**
  - 12:    $\beta^{t+1} = \Pi \left( \Omega - \mathbf{c}^\top \mathbf{u}^{t+1} - \frac{1}{\rho} \lambda_6^t \right)_{\mathbb{R}_+}$
  - 13:    $\boldsymbol{\lambda}_1^{t+1} = \boldsymbol{\lambda}_1^t + \rho (\mathbf{S}^{t+1} \mathbf{1} - \mathbf{u}^{t+1})$
  - 14:    $\boldsymbol{\lambda}_2^{t+1} = \boldsymbol{\lambda}_2^t + \rho (\mathbf{W}^{t+1} \mathbf{1} - \mathbf{1})$
  - 15:    $\boldsymbol{\lambda}_3^{t+1} = \boldsymbol{\lambda}_3^t + \rho (\mathbf{D} \mathbf{u}^{t+1} - \mathbf{q})$
  - 16:    $\boldsymbol{\lambda}_4^{t+1} = \boldsymbol{\lambda}_4^t + \rho (\mathbf{A} \mathbf{u}^{t+1} - \boldsymbol{\gamma}^{t+1})$
  - 17:    $\boldsymbol{\Lambda}_5^{t+1} = \boldsymbol{\Lambda}_5^t + \rho (\mathbf{H}^{t+1} - \mathbf{S}^{t+1})$
  - 18:    $\lambda_6^{t+1} = \lambda_6^t + \rho (\mathbf{c}^\top \mathbf{u}^{t+1} + \beta^{t+1} - \Omega)$
  - 19:    $\boldsymbol{\Lambda}_7^{t+1} = \boldsymbol{\Lambda}_7^t + \rho (\mathbf{W}^{t+1} - \mathbf{S}^{t+1})$
  - 20: **end for**
  - 21: **Return:**  $\mathbf{S}^{\tilde{T}}$
- 

In Algorithm 1,  $\Pi(\cdot)_{[0,1]}$  is the operator that projects each entry of the input matrix to the interval  $[0, 1]$  and  $\Pi(\cdot)_{\mathbb{R}_+}$  is the operator that projects each entry of the input matrix on to  $\mathbb{R}_+$ . In Algorithm 1 steps 4, 5, and 6 are computationally cumbersome due to the size of the matrices  $\mathbf{W}$ ,  $\mathbf{H}$ , and  $\mathbf{S}$ . However, each column of the matrices

$\mathbf{W}$ ,  $\mathbf{H}$ , and  $\mathbf{S}$  corresponds to a single driver and hence the computation corresponding to each column can be performed in parallel on smartphone devices of the drivers. Moreover, since the steps are not coupled, they can be solved in parallel on the drivers' smart devices. Further details about the steps of a distributed computation of Algorithm 1 are provided in Appendix C. Theorem 1 guarantees the convergence of our ADMM algorithm.

*Theorem 1:* Algorithm 1 finds an  $\epsilon$ -optimal solution of problem (8) in  $O(1/\epsilon)$  iterations [74].

Theorem 1 guarantees the convergence of Algorithm 1 that is provided for optimization problem (8). The optimization problem (8) is a (convex) reformulation of the relaxed problem (7), and is amenable to ADMM. However, as it was mentioned, the original problem (6) is likely hard to solve since it is a special instance of polynomial optimization with discrete variables and function  $f$  does not seem to have any special structure to reduce its complexity.

In optimization problem (7) (and consequently (8)), all solutions  $\mathbf{S}^*$  with a fixed value of  $\mathbf{S}^* \mathbf{1} = \mathbf{u}^*$  lead to the same objective as long as  $\mathbf{S}^{*\top} \mathbf{1} = \mathbf{1}$ . Hence, this convex problem can have an infinite number of solutions (with many of them not even close to binary). Therefore, in order to find (approximately) binary solutions, we add the following regularizer to the objective function in (8):

$$\mathfrak{R}(\mathbf{H}_{r,i,n}) = -\frac{\tilde{\lambda}}{2} \mathbf{H}_{r,i,n} (\mathbf{H}_{r,i,n} - 1) \quad (9)$$

where  $\tilde{\lambda} \in \mathbb{R}_+$  is the regularization parameter and  $\mathbf{H}_{r,i,n} \in [0, 1]$ . This regularizer forces the elements of matrix  $\mathbf{H}$  to be as close as possible to the binary domain  $\{0, 1\}$ .

While Algorithm 1 returns the solution of the optimization problem (8), this problem (8) is a relaxation of the original problem (6). Hence, the obtained solution in Algorithm 1 must be utilized to obtain a feasible point in (6). For this step, we solve the following mixed integer (linear) problem

$$\begin{aligned} \min_{\mathbf{S}} \quad & \|\mathbf{S}\mathbf{1} - \mathbf{u}^*\|_1 \\ \text{s.t.} \quad & \mathbf{S}^\top \mathbf{1} = \mathbf{1}, \quad \mathbf{c}^\top \mathbf{S}\mathbf{1} \leq \Omega \\ & \mathbf{D}\mathbf{S}\mathbf{1} = \mathbf{q}, \quad \mathbf{S} \in \{0, 1\}^{(|\mathcal{R}||\mathcal{Z}|) \times |\mathcal{N}|} \end{aligned} \quad (10)$$

where  $\mathbf{u}^*$  is the optimal solution obtained by Algorithm 1. We can use off-the-shelf solvers such as Gurobi to solve (10).

The BPR function of Algorithm 1 in Section II-A can capture both Scenario I in Section II-A and Scenario II in Section II-B. However, the computational requirements for the free-flow case in Scenario I in Section II-A are less expensive compared to that of the congested case in Scenario II in Section II-B. Thus, model (3) in Scenario I in Section II-A is an alternative when computational resources are limited.

### III. NUMERICAL EXPERIMENTS

We evaluate the performance of our algorithms using data from the Los Angeles area. The Los Angeles region is ideally suited for being the validation area because there are multiple routes connecting most OD pairs. Additionally, researchers at the University of Southern California have developed the Archived Data Management System (ADMS)

that collects, archives, and integrates a variety of transportation datasets from Los Angeles, Orange, San Bernardino, Riverside, and Ventura Counties. ADMS includes access to real-time traffic data from 9500 highway and arterial loop detectors with measurements every 30 seconds and 1 minute respectively.

Due to the lack of access to the drivers' routing information, we need to estimate the origin-destination (OD) matrix from the network flow information. Rows and columns of the OD matrix correspond to the origin and destination points respectively. For OD matrix  $A$ , the element  $A_{(i,j)}$  is the number of drivers going from point  $i$  to point  $j$ . The OD matrix estimation problem is under-determined [75–77]. There are two categories of OD matrices: static and dynamic [78]. Due to the high resolution of our data, most of the existing dynamic OD estimation (DODE) methods become computationally inefficient. In addition, we do not have prior data of the OD matrix which many studies consider as given data [79–82] and we do not have access to prior observations of the OD matrix. Given these barriers, we relied on the algorithm proposed by [57]. This algorithm performs without employing any prior OD matrix information.

### A. Simulation Model

In our numerical experiments, we integrate different datasets and models to evaluate the performance of our algorithms. First, we extract the speed data, volume data, and sensor information including the location of sensors from the Archived Data Management System (ADMS). Then, we use the distances of sensors, extracted from the location of sensors using Google Maps API, to create the graph of the network. We created three sets of graph networks corresponding to the regions depicted in Fig. 1, Fig. 3, and Fig. 4. In the next step, the speed data, volume data, and the network graph are used for estimating OD pairs by the algorithm provided in [57]. The total number of estimated incoming drivers for all three experiments is presented in Fig. 5. For each OD pair, we find up to 4 different routing options. In particular, we start by the shortest path for each OD pair. Then, we remove the edges in this path and go with the second shortest path, and we continue this process until we find 4 different routes between the origin and destination (or no other routes exist). We use the model in [55] to compute the acceptance probability for the different offers on the different routes for each individual driver. The parameters used for computing the probability are static values provided by [55] and we only calibrate some of the parameters because we are only using historical data and we do not have access to the drivers' features such as age or gender. In this paper, we do not learn the route choice model of the drivers so the parameters of the probability model are fixed but it is possible to adapt our routing model to the drivers' preferences by observing the drivers' behavior. We run three different experiments that model the road network at different scales. In Experiment I, we model an arterial region (Fig. 1) but includes surface streets. For Experiment II, we model a large network of highways (Fig. 3). For Experiment III, we model a moderate region (Fig. 4) which is a subset of the region in Experiment II. We use travel time savings as our metric for performance evaluation in all experiments. Besides travel time savings, we also include the monetary value of traffic reduction based on the Value of Time (VOT) as an alternative metric. Our base Value of Time (VOT) is derived from the estimation of [83] which is \$2.63 per minute or \$157.8 per hour.

To solve model (3), we use the Gurobi solver in all experiments. Also, we solve model (6) in Experiment III utilizing Gurobi and MOSEK to compare their results with Algorithm 1 [84]. The comparison between ADMM,

Gurobi, and MOSEK is shown in Experiment III. Gurobi and MOSEK are state-of-the-art off-the-shelf commercial solvers of linear and mixed integer optimization problems. To better balance accuracy and the required time for solving the problem, we set the relative mixed integer programming optimality gap at 0.01 for both Gurobi and MOSEK in the experiments. Given that ADMM is also known to satisfy the constraints “asymptotically”, we need to evaluate the solution quality after terminating our algorithm in a finite many number of iterations. We have measured the quality of our ADMM-based algorithm by computing the normalized gap error between the right-hand side and the left-hand side of our constraints as

$$f_{gap}(\mathbf{S}, \mathbf{u}, \mathbf{W}, \mathbf{H}, \beta, \gamma) = \frac{\|\mathbf{S}\mathbf{1} - \mathbf{u}\|}{\|\mathbf{S}\| \|\mathbf{1}\| + \|\mathbf{u}\|} + \frac{\|\mathbf{W}^\top \mathbf{1} - \mathbf{1}\|}{\|\mathbf{W}^\top\| \|\mathbf{1}\| + \|\mathbf{1}\|} + \frac{\|\mathbf{D}\mathbf{u} + \mathbf{q}\|}{\|\mathbf{D}\| \|\mathbf{u}\| + \|\mathbf{q}\|} + \frac{\|\mathbf{A}\mathbf{u} - \gamma\|}{\|\mathbf{A}\| \|\mathbf{u}\| + \|\gamma\|} \\ + \frac{\|\mathbf{H} - \mathbf{S}\|}{\|\mathbf{H}\| + \|\mathbf{S}\|} + \frac{\|\mathbf{W} - \mathbf{S}\|}{\|\mathbf{W}\| + \|\mathbf{S}\|} + \frac{\|\mathbf{c}^\top \mathbf{u} + \beta - \Omega\|}{\|\mathbf{c}^\top\| \|\mathbf{u}\| + \|\beta\| + \|\Omega\|}.$$

While we only provide incentives to the drivers that enter the system in the first time interval, our incentive offering mechanism considers estimations of the traffic flows in the next time intervals. The selected drivers for incentivization are from the same cohort. We randomly select a group of drivers between 7 AM and 7:15 AM. Then, we use the selected drivers to compare the performance of the model with different budget values on the total travel time for 7 AM to 8 AM. While our formulation is static, it can be applied in a dynamic environment if solved frequently in the network in order to offer incentives to the drivers.

To evaluate the travel time of the network, we use the volume of the network at the User Equilibrium (UE) after the incentivization. After the incentivization, the user drivers that have accepted the incentive offer cannot change their incentivized route as part of the assumed incentivization policy. However, the remainder of the drivers (user drivers that rejected the incentive offer, user drivers that did not receive an incentive offer, and nonuser drivers) can select their route based on the new traffic volume at the UE resulting from the incentivization. In other words, our framework does not assume that drivers who are not incentivized will remain on the previous routes. Hence, those who are not incentivized may also change routes as the traffic conditions change due to the incentives. To compute the total travel time at the UE, we provide Algorithm 2 in Appendix C. Algorithm 2 returns the total travel time of the system at UE given the routing assignment of incentivized drivers who accepted the incentive offer and the OD information of the remaining drivers. The decision of the incentivized driver on accepting/rejecting the offer is randomly made based on the probability of their acceptance given the incentive offer.

### B. Experiment I

In Experiment I, we check the performance of model (3) using the ADMS data for May 5<sup>th</sup>, 2018 with the incentive set  $\mathcal{I} = \{\$0, \$2, \$10\}$ . The studied region, which is depicted in Fig. 1, includes the data of 301 sensors. Based on the ADMS data, we created a graph with 41 nodes, 139 links, and 105.5 miles of road. OD points are located at intersections and close to the ramp of the highways. The number of OD pairs is 1681 and there are 4278 paths between them in total. We assume 7494 drivers enter the system between 7 AM and 8 AM and we consider 1805 drivers entering the system in the first 15 minutes for incentivization. To evaluate the travel time of the network, we run Algorithm 2 with step size  $\alpha_{UE} = 0.05$  and  $\tilde{T} = 20$  iterations and report the travel time at UE after the incentivization.



Fig. 1. Studied region in Experiment I.

	Budget (\$)			
	0	100	1000	10000
Cost (\$)	0	100	1000	9996
Value of saved time (\$)	0	729	4320	7471
Total travel time (hour)	679	674	652	632

TABLE I  
EXPERIMENT I: LINEAR MODEL (3).

Notice that model (3) may result in an infeasible optimization problem (particularly in a heavily congested network). Hence, we included a parameter  $\alpha$  in our formulation as the multiplier of the allowed capacity. In other words, we use  $\alpha \times v_0$  instead of  $v_0$  in model (3). We only consider this multiplier during the computation of incentives; however, during the computation of total travel time, we use the original capacity. We assumed zero dollar incentive in our probabilistic model for drivers that are not receiving an incentive.

Results of model (3) at 100% penetration rate (percentage of drivers who are considered in incentivization) are presented in TABLE I. In this table, “Total travel time” shows the travel time computed via the BPR function after offering incentives. When the budget is increased from \$1000 to \$10,000, the percentage of total travel time decrease is improved from 4.03% to 6.97%. The row “Cost” in the table shows the amount of the budget that was used. In all cases, almost all of the budget is used. The results show that the value of saved time is much larger than the amount spent on incentive except in the budget of \$10,000. Note that a budget of zero is the case of no incentive.

TABLE II shows that increasing the budget results in higher percentage of drivers to whom we offered the

Number of drivers entering the system	Budget (\$)	% of rewarded drivers	Average incentive amount	Reduction in total travel time
7402	1000	6.67%	\$2.00	4.03%
	10000	13.64%	\$9.78	6.97%

TABLE II  
COMPARISON OF \$1000 AND \$10000 BUDGET IN EXPERIMENT I.

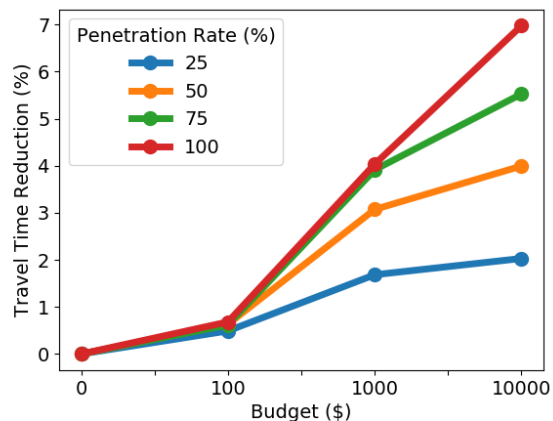


Fig. 2. Effect of the penetration rate on the percentage of travel time decrease in Experiment I.

incentive and a higher average amount of offered incentives. In addition, we observe that even offering incentives to 6.67% of the drivers (with an average of \$2.00 monetary incentive per driver) can reduce the total travel time by 4.03%. If approximately 13.64% of the drivers are incentivized with an average of \$9.78 per driver, the total travel time can be reduced by almost 6.97%. For more details about the distribution of offered incentives to drivers in Experiment I, please see TABLE X in the Appendix.

Fig. 2 shows the effect of the penetration rate on travel time decrease. By reducing the penetration rate, we experience a smaller travel time decrease because the flexibility of the model in selecting drivers decreases. Although reducing the penetration rate adversely affects the incentivization, the model focuses on available drivers for reducing travel time. For more details on the numbers provided in Fig. 2, please see TABLE XVIII and TABLE XVII in the Appendix.

### C. Experiment II

In Experiment II, we evaluate the performance of our methods for the region depicted in Fig. 3 with 753 sensors under two different possible sets of incentives:

- $\mathcal{I}_1 = \{\$0, \$2, \$10\}$
- $\mathcal{I}_2 = \{\$0, \$1, \$2, \$3, \$5, \$10\}$

This region only includes data of highway sensors with 25 OD points and 32 links which includes 707.6 miles of road. The number of OD pairs is 625, and there are 1331 paths between them in total. We assume 15093 drivers enter the system between 7 AM and 8 AM. Our incentivization model considers 4126 drivers entering the system in the first 15 minutes. To evaluate the travel time of the network, we run Algorithm 2 following the same settings as Experiment I. The results of our experiment at 100% penetration rate are presented in TABLE III for incentive set  $\mathcal{I}_1$ , and in TABLE IV for incentive set  $\mathcal{I}_2$ . The value of saved time is much larger than the cost of offering incentives for all budget values for both incentive sets except in the budget of 10,000. The value of saved time can go up to 15 times the cost.



Fig. 3. Studied region in Experiment II.

	Budget (\$)			
	0	100	1000	10000
Cost (\$)	0	100	1000	9998
Value of saved time (\$)	0	1430	3955	8519
Total travel time (hour)	4253	4244	4228	4199

TABLE III  
EXPERIMENT II: LINEAR MODEL (3) FOR INCENTIVE SET  $\mathcal{I}_1$ .

	Budget (\$)			
	0	100	1000	10000
Cost (\$)	0	100	1000	10000
Value of saved time (\$)	0	1546	3931	9741
Total travel time (hour)	4253	4243	4228	4191

TABLE IV  
EXPERIMENT II: LINEAR MODEL (3) FOR INCENTIVE SET  $\mathcal{I}_2$ .

	Number of drivers entering the system	Budget (\$)	% of rewarded drivers	Average incentive amount	Reduction in total travel time
Exp. II-1	15093	1000	2.97%	\$2.23	0.59%
		10000	16.42%	\$4.03	1.27%
Exp. II-2	15093	1000	3.87%	\$1.71	0.59%
		10000	15.97%	\$4.15	1.45%

TABLE V  
COMPARISON OF \$1000 AND \$10000 BUDGET IN EXPERIMENT II.



Fig. 4. Studied region in Experiment III.

In addition to confirming our previous observations in Experiment I, Experiment II shows the diversity gain related to the incentive set  $\mathcal{I}_1$  (see the “Reduction in total travel time” column in TABLE V). In other words, more choices in the incentive set provides more flexibility for the algorithm, resulting in a total travel time reduction. For more details about the distribution of offered incentives to drivers in Experiment II, please see TABLE XI and TABLE XII in the Appendix. By examining Experiments I and II, we observe that more alternative routes leads to more gain in the travel time reduction.

#### D. Experiment III

In Experiment III, we compare the performance of the linear model (3) and the ADMM model (6) using the incentive set  $\mathcal{I} = \{\$0, \$2, \$10\}$ . The region considered in our analysis is depicted in Fig. 4. This region includes the data of 293 sensors. Based on the ADMS data, we created a graph with 12 nodes, 32 links, and 288.1 miles of road. The number of OD pairs is 144 and there are 270 paths between them in total. The estimated total number of drivers incoming to the system between 5 AM to 9 AM by the OD estimation algorithm is depicted in Fig. 5 (c). In our simulations, we assume 8220 drivers enter the system between 7 AM and 8 AM. Our incentivization model considers 2248 drivers entering the system in the first 15 minutes. To evaluate the travel time of the network, we run Algorithm 2 following the same settings as Experiment I. Results of model (3) and model (6) at 100% penetration rate are presented in TABLE VI and Fig. 6.

As we can observe in TABLE VII and Fig. 6, model (6) has a better performance compared to model (3) for all the budgets. At 100% penetration rate, model (6) decreased the travel time up to twice model (3). Although the objective function in model (3) reduces the total free flow travel time, the actual travel time is not reached since the free flow travel time is a poor estimation of the actual travel time. Model (6) directly minimizes the travel time based on the BPR function so it captures the nonlinear relation between travel time and volume. When the volume is greater than the capacity, model (6) which is a more accurate model representing the traffic network produces better results. These phenomena can be observed in Fig. 6, Fig. 7, Fig. 8, and Fig. 8. Although both Gurobi and MOSEK find slightly better solutions for model (6), it can take up to 35 hours for Gurobi and up to 80 hours for MOSEK to solve the problem. However, Algorithm 1 takes at most 14 minutes by utilizing parallel computation. Also, our computational resources were limited. With a proper use of GPUs and TPUs, matrix computations can be

		Budget (\$)			
		0	100	1000	10000
Model (3) (Linear)	Cost (\$)	0	100	1000	10000
	Value of saved time (\$)	0	604	6550	9760
	Total travel time (hour)	2087	2082	2045	2024
Model (6) (ADMM)	Cost (\$)	0	100	1000	9578
	Value of saved time (\$)	0	1204	8999	15149
	Total travel time (hour)	2087	2079	2029	1990

TABLE VI  
EXPERIMENT III: LINEAR MODEL (3) AND MODEL (6).

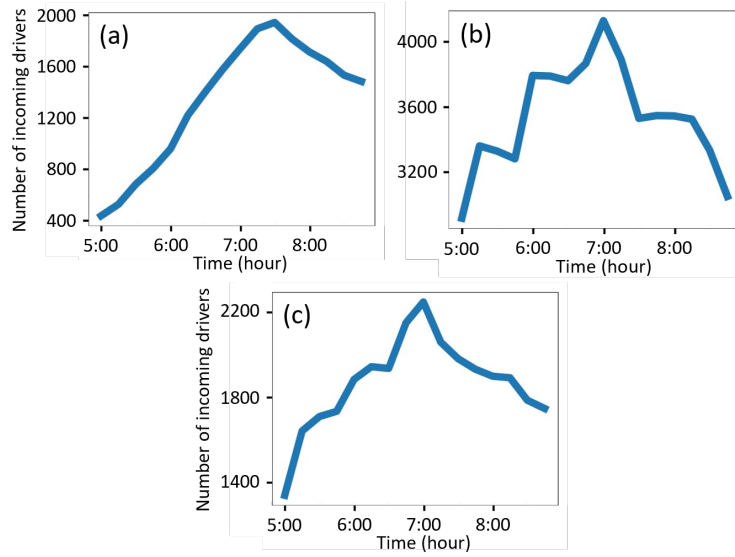


Fig. 5. Total estimated number of drivers entering the system (in 15-minute intervals). (a) Experiment I, (b) Experiment II, and (c) Experiment III.

	Number of drivers entering the system	Budget (\$)	% of rewarded drivers	Average incentive amount	Reduction in total travel time
Exp. III Model (3)	8220	1000	6.08%	\$2.00	1.99%
		10000	15.86%	\$7.67	2.96%
Exp. III Alg. 1	8220	1000	6.08%	\$2.00	2.73%
		10000	14.46%	\$8.06	4.60%

TABLE VII  
COMPARISON OF \$1000 AND \$10000 BUDGET IN EXPERIMENT III.

even much more efficient. We set the termination rule of MOSEK and Gurobi as 0.01 relative optimality gap. Also, we have computed the normalized gap error of our ADMM-based Algorithm 1 to measure the quality of its solution. This error is illustrated in Figure 10 for Experiment III after 50,000 iterations for different penetration rates and budgets in Figure 10. We can observe that the error after 10,000 iterations converges almost to 0 for most of the cases and after 20,000 iterations, it converges almost to 0 for all the cases.

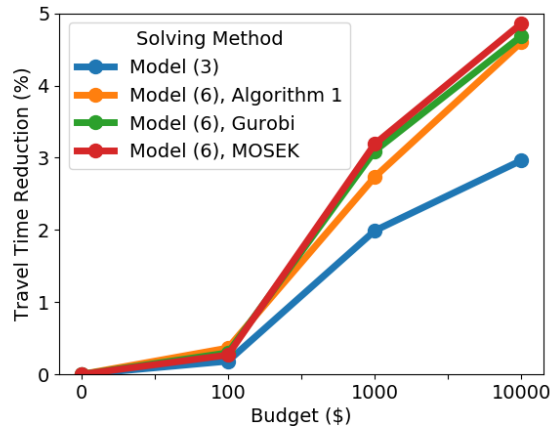


Fig. 6. Effect of solving method on the percentage of travel time decrease in Experiment III.

Algorithm 1 by offering incentives to 14.46% of the vehicles at 100% penetration rate in Experiment III (with an average of \$8.06 monetary incentive per driver) can reduce the total travel time by 4.60% using model (6). For a budget of \$10,000, model (6) has 1.64% larger reduction in the percentage of travel time compared to model (3) although both offer almost the same amount of incentive on average to the almost same percentage of drivers. The computation time of model (3) is 2.6 minutes, but model (6) requires up to 1.04 hours to run if we employ serial computation. Utilizing parallel computation as described in section II-C, we can reduce the computational time to at most 14 minutes. The value of saved time using Algorithm 1 is much larger than the amount spent on incentive for all budget values and it can go up to 12 times the cost. For more details about the distribution of the offered incentives to the drivers in Experiment III, please see TABLE XIII, TABLE XIV, and TABLE XV in the Appendix. The effect of the penetration rate on travel time decrease in Experiment III for model (6) is depicted in Fig. 7, Fig. 8, and Fig. 9. The behavior is similar to our observation in Fig. 2 which was for Model (3). For more details of the numbers provided in Fig. 7, Fig. 8, and Fig. 9, please see TABLE XX, TABLE XIX, TABLE XXII, TABLE XXI, TABLE XXIV, and TABLE XXIII in the Appendix.

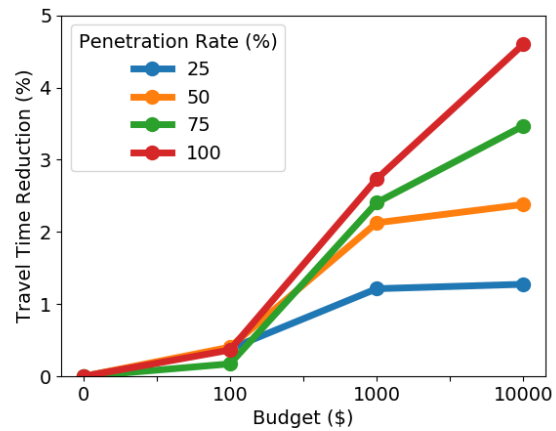


Fig. 7. Effect of the penetration rate on the percentage of travel time decrease in Experiment III, model (6), Algorithm 1.

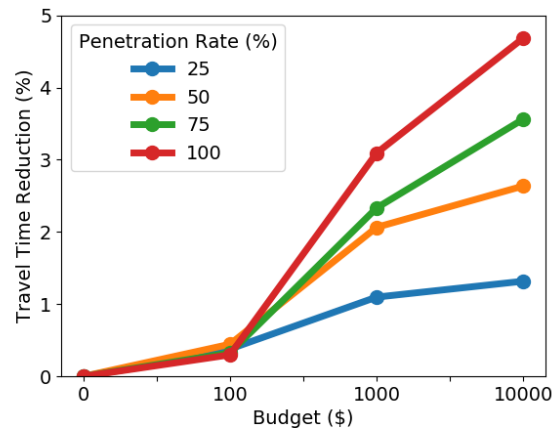


Fig. 8. Effect of the penetration rate on the percentage of travel time decrease in Experiment III, model (6), Gurobi solver.

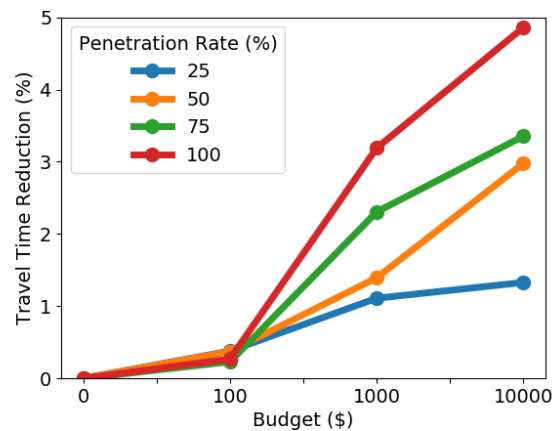


Fig. 9. Effect of the penetration rate on the percentage of travel time decrease in Experiment III, model (6), MOSEK solver.

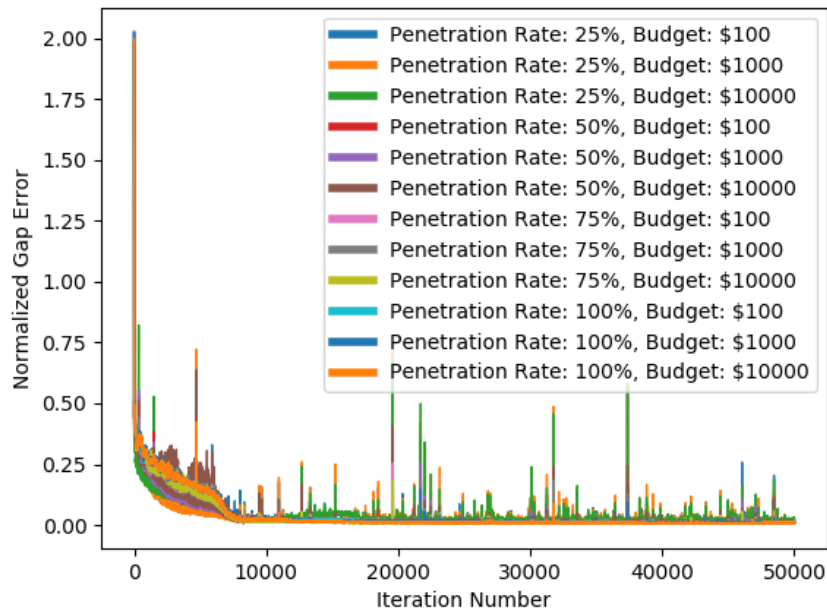


Fig. 10. Normalized gap error of Algorithm 1 after 50,000 iterations with different cases of penetration rate and budget.

### E. Summary

As we discussed in section II-A, model (3) assumes that there exists a traffic flow solution operating below the network capacity. When this assumption is not satisfied, our model results in an “approximate” solution. To evaluate the validity of this approximation in heavily congested networks, we ran model (3) for heavily congested networks (Experiments I and II) with many alternative routes so that we can reasonably reduce the congestion level. As we saw in Experiments I and II, this model can provide a reasonable approximation in both arterial (Experiment I) and highways (Experiment II) and leads to congestion reduction even when the final result is above the system capacity. In Experiment III, our numerical experiments demonstrate the superiority of model (6) over model (3) in reducing congestion. This is because of the heavy congestion and the lack of availability of enough alternative routes to reduce congestion (so that the final solution of model (3) is far away from the free flow traffic and a linear approximation of travel time is no longer accurate enough). We were not able to run model (6) for Experiments I and II due to the large number of nodes in the network. However, relying on edge computation, this model could be solved efficiently in practice as we discussed in subsection II-C.

## IV. CONCLUSION

In this paper, we developed mathematical models and proposed algorithms for offering personalized incentives to drivers to reduce congestion in the network. In this framework, drivers share their origin-destination and routing information with a central planner. Based on this information, the central planner then offers incentives to drivers to incentivize/enforce a socially optimal routing strategy. The incentives are offered based on solving large-scale optimization problems in our framework. In our framework, we bring together prior works to model the behavior of

drivers in response to the offered incentives as well as the resulting congestion reduction in the network where no traffic control is required. We paid special attention to minimizing the total travel time of the network. In addition, we showed that this problem can be solved in a distributed fashion where some of the computations are performed on individual drivers' smart devices. Finally, we evaluated the performance of our models and algorithms using Archived Data Management System (ADMS) data. Our experiments showed that the proposed framework can lead up to a 5% decrease in the total travel time of the system during rush hour times.

In this work, the incentives are only offered to alter the routing decision of the drivers. In future work, it is crucial to look at the effect of offering incentives to change the mode or time of the drivers' trips. These options will bring additional flexibility to the model, which in turn will result in further congestion reduction. To compute the drivers' acceptance probability, we can include more aspects of drivers' characteristics and features into account such as gender, age, and salary. In addition, we can utilize preference learning in computing drivers' acceptance probability if we have access to the data of preferences of the drivers. Moreover, future research can study the use of more realistic approaches such as using a dynamic route assignment approach or using a cost flow curve with a vertical asymptote at capacity.

## V. ACKNOWLEDGEMENT

This work was funded by a grant from the National Center for Sustainable Transportation (NCST), supported by the U.S. Department of Transportation's University Transportation Centers Program (Caltrans 65A0686 Task Order 043; USDOT Grant 69A35).

## APPENDIX A

### LIST OF NOTATIONS

The following symbols are used in this paper.

- $\mathcal{G}$ : Directed graph of the traffic network
- $\mathcal{V}$ : Set of nodes of graph  $\mathcal{G}$  which correspond to major intersections and ramps
- $\mathcal{E}$ : Set of edges of graph  $\mathcal{G}$  which correspond to the set of road segments
- $|\mathcal{E}|$ : Total number of road segments/edges in the network  $\mathcal{G}$  (i.e. the cardinality of the set  $\mathcal{E}$ )
- $\mathbf{r}$ : Route vector
- $\mathbf{T}$ : Time horizon
- $|\mathbf{T}|$ : Number of time units (i.e. the cardinality of  $\mathbf{T}$ )
- $\mathbf{v}_0$ : Capacity vector of road segments
- $\mathbf{v}_t$ : Volume vector of road segments at time  $t$
- $\mathcal{N}$ : Set of drivers
- $|\mathcal{N}|$ : Number of drivers (i.e. the cardinality of the set  $\mathcal{N}$ )
- $\mathcal{R}_n$ : Set of possible route options for driver  $n$
- $\mathcal{R}$ : Total set of possible route options for all drivers
- $|\mathcal{R}|$ : Number of possible route options (i.e. the cardinality of the set  $\mathcal{R}$ )

- $\mathcal{I}_n$ : Set of possible incentives to offer to driver  $n$
- $\mathcal{I}$ : Total set of possible incentives to all drivers
- $|\mathcal{I}|$ : Number of possible incentives (i.e. the cardinality of the set  $\mathcal{I}$ )
- $s_i^{r,n}$ : Decision parameter indicates whether incentive  $i$  is offered to driver  $n$  for route  $\mathbf{r}$
- $p_i^{r,n}$ : The probability of acceptance of route  $\mathbf{r}$  by driver  $n$  given incentive  $i$
- $\hat{T}_{\mathbf{r}}$ : The estimate of the travel time for route  $\mathbf{r}$  provided by the incentive offering platform
- $T_{\mathbf{r}}$ : The exact travel time for route  $\mathbf{r}$
- $\beta_{\mathbf{r},t}$ : The vector of the location of driver that is traveling a route  $\mathbf{r}$  at time  $t$
- $\eta_i$ : The cost of incentive  $i$
- $F_{tt}(\cdot)$ : Total travel time function
- $\delta_{\ell,t}$ : Travel time of link  $\ell$  at time  $t$
- $\hat{\mathbf{v}}$ : The vector of the volume of links at different times in the horizon
- $\hat{v}_{\ell,t}$ : The  $(|\mathcal{E}| \times t + \ell)^{th}$  element of vector  $\hat{\mathbf{v}}$  representing the volume of  $\ell^{th}$  link at time  $t$
- $t_0$ : The free flow travel time of the link
- $v$ : The traffic volume of the link
- $w$ : The practical capacity of the link
- $\mathbf{s}_n$ : The binary decision vector for one driver in which only one element has the value of one and it corresponds to the route and the incentive amount that we offer
- $f_{\text{BPR}}(\cdot)$ : BPR function
- $\mathbf{S}$ : Decision matrix
- $\mathbf{R}$ : The matrix of the location of a driver
- $\mathbf{P}$ : Route choice probability matrix
- $\mathbf{D}$ : The matrix of incentive assignment to OD pairs
- $\mathbf{q}$ : The vector of the number of drivers for each OD pair
- $\mathbf{c}$ : The vector of cost of incentives assigned to each route
- $\Omega$ : Budget
- $\omega$ : The vector of free flow travel time of links
- $\mathbf{a}_{\ell,t}$ : The row of matrix  $\mathbf{A} = \mathbf{R}\mathbf{P}$  which corresponds to link  $\ell$  at time  $t$
- $K$ : The number of OD pairs
- $e$ : An edge of graph  $\mathcal{G}$  which corresponds to a road segments in the traffic network

## APPENDIX B

### DETAILS OF ALTERNATING DIRECTION METHOD OF MULTIPLIERS (ADMM)

Before explaining the steps of our proposed algorithm, let us first explain the Alternating Direction Method of

Multipliers (ADMM), which is the main building block of our framework.

#### A. Review of ADMM

ADMM developed in [63] and [64] aims at solving linearly constrained optimization problems of the form

$$\min_{w,z} h(w) + g(z) \quad \text{s.t.} \quad Aw + Bz = c,$$

where  $w \in \mathbb{R}^{d_1}$ ,  $z \in \mathbb{R}^{d_2}$ ,  $c \in \mathbb{R}^k$ ,  $A \in \mathbb{R}^{k \times d_1}$ , and  $B \in \mathbb{R}^{k \times d_2}$ . By forming the augmented Lagrangian function

$$\mathcal{L}(w, z, \lambda) \triangleq h(w) + g(z) + \langle \lambda, Aw + Bz - c \rangle + \frac{\rho}{2} \|Aw + Bz - c\|_2^2,$$

each iteration of ADMM applies alternating minimization to the primal variables and gradient ascent to the dual variables:

$$\begin{aligned} \text{Primal Update:} \quad & w^{r+1} = \arg \min_w \mathcal{L}(w, z^r, \lambda^r), \\ & z^{r+1} = \arg \min_z \mathcal{L}(w^{r+1}, z, \lambda^r) \\ \text{Dual Update:} \quad & \lambda^{r+1} = \lambda^r + \rho (Aw^{r+1} + Bz^{r+1} - c) \end{aligned} \quad (11)$$

This algorithm is well studied in the optimization literature (see [62] for a monograph on the use of this algorithm in convex distributed optimization and [65] for its use in non-convex continuous optimization).

#### B. ADMM for Solving (7)

To follow the standard form provided at subsection B-A and substitute  $\mathbf{a}_{\ell,t} \mathbf{S} \mathbf{1}$  with  $\gamma_{\ell,t}$ , we reformulate the optimization problem (7) as

$$\begin{aligned} \min_{\mathbf{S}, \gamma, \beta} \quad & F_{tt}(\gamma) = \sum_{\ell=1}^{|\mathcal{E}|} \sum_{t=1}^{|\mathbf{T}|} (\gamma_{\ell,t}) \delta(\gamma_{\ell,t}) \\ \text{s.t.} \quad & \mathbf{S}^\top \mathbf{1} = \mathbf{1}, \quad \mathbf{c}^\top \mathbf{S} \mathbf{1} + \beta = \Omega \\ & \mathbf{D} \mathbf{S} \mathbf{1} = \mathbf{q}, \quad \mathbf{A} \mathbf{S} \mathbf{1} = \gamma \\ & \mathbf{S} \in [0, 1]^{(|\mathcal{R}| \cdot |\mathcal{I}|) \times |\mathcal{N}|}, \quad \beta \geq 0 \end{aligned} \quad (12)$$

where  $\beta$  is a slack variable. As we discussed in subsection II-C, in order to find (approximately) binary solutions, we add a regularizer  $\mathfrak{R}(\mathbf{S}) = -\frac{\tilde{\lambda}}{2} \sum_{r=1}^{|\mathcal{R}|} \sum_{i=1}^{|\mathcal{I}|} \sum_{n=1}^{|\mathcal{N}|} \mathbf{S}_{r,i,n} (\mathbf{S}_{r,i,n} - 1)$  to the objective function:

$$\begin{aligned} \min_{\mathbf{S}, \gamma, \beta} \quad & F_{tt}(\gamma) = \sum_{\ell=1}^{|\mathcal{E}|} \sum_{t=1}^{|\mathbf{T}|} (\gamma_{\ell,t}) \delta(\gamma_{\ell,t}) \\ & - \frac{\tilde{\lambda}}{2} \sum_{r=1}^{|\mathcal{R}|} \sum_{i=1}^{|\mathcal{I}|} \sum_{n=1}^{|\mathcal{N}|} \mathbf{S}_{r,i,n} (\mathbf{S}_{r,i,n} - 1) \\ \text{s.t.} \quad & \mathbf{S}^\top \mathbf{1} = \mathbf{1}, \quad \mathbf{c}^\top \mathbf{S} \mathbf{1} + \beta = \Omega \\ & \mathbf{D} \mathbf{S} \mathbf{1} = \mathbf{q}, \quad \mathbf{A} \mathbf{S} \mathbf{1} = \gamma \\ & \mathbf{S} \in [0, 1]^{(|\mathcal{R}| \cdot |\mathcal{I}|) \times |\mathcal{N}|}, \quad \beta \geq 0 \end{aligned} \quad (13)$$

where  $\tilde{\lambda} \in \mathbb{R}_+$  is the regularization parameter. This regularizer forces the elements of matrix  $\mathbf{S}$  to be as close as possible to the binary domain  $\{0, 1\}$ . The augmented lagrangian of the reformulated optimization problem (13) is

$$\begin{aligned}
& \mathcal{L}(\mathbf{S}, \boldsymbol{\gamma}, \beta) \\
& \triangleq F_{tt}(\boldsymbol{\gamma}) + \mathbb{I}_{[0,1]^{(|\mathcal{R}| \cdot |\mathcal{I}|) \times |\mathcal{N}|}}(\mathbf{S}) + \mathbb{I}_{\mathbb{R}^+}(\beta) \\
& \quad - \frac{\tilde{\lambda}}{2} \sum_{r=1}^{|\mathcal{R}|} \sum_{i=1}^{|\mathcal{I}|} \sum_{n=1}^{|\mathcal{N}|} \mathbf{S}_{r,i,n} (\mathbf{S}_{r,i,n} - 1) \\
& \quad + \langle \boldsymbol{\lambda}_1, \mathbf{S}^\top \mathbf{1} - \mathbf{1} \rangle + \lambda_2 (\mathbf{c}^\top \mathbf{S} \mathbf{1} + \beta - \Omega) \\
& \quad + \langle \boldsymbol{\lambda}_3, \mathbf{D} \mathbf{S} \mathbf{1} - \mathbf{q} \rangle + \langle \boldsymbol{\lambda}_4, \mathbf{A} \mathbf{S} \mathbf{1} - \boldsymbol{\gamma} \rangle \\
& \quad + \frac{\rho}{2} \|\mathbf{S}^\top \mathbf{1} - \mathbf{1}\|^2 + \frac{\rho}{2} (\mathbf{c}^\top \mathbf{S} \mathbf{1} + \beta - \Omega)^2 \\
& \quad + \frac{\rho}{2} \|\mathbf{D} \mathbf{S} \mathbf{1} - \mathbf{q}\|^2 + \frac{\rho}{2} \|\mathbf{A} \mathbf{S} \mathbf{1} - \boldsymbol{\gamma}\|^2
\end{aligned} \tag{14}$$

with the set of Lagrange multipliers  $\{\boldsymbol{\lambda}_1, \lambda_2, \boldsymbol{\lambda}_3, \boldsymbol{\lambda}_4\}$  and  $\rho > 0$  be the primal penalty parameter. Then, ADMM solves (13) by the following iterative scheme

$$\begin{aligned}
\mathbf{S}^{t+1} &= \underset{\mathbf{S}}{\operatorname{argmin}} \quad \mathbb{I}_{[0,1]^{(|\mathcal{R}| \cdot |\mathcal{I}|) \times |\mathcal{N}|}}(\mathbf{S}) \\
& \quad - \frac{\tilde{\lambda}}{2} \sum_{r=1}^{|\mathcal{R}|} \sum_{i=1}^{|\mathcal{I}|} \sum_{n=1}^{|\mathcal{N}|} \mathbf{S}_{r,i,n} (\mathbf{S}_{r,i,n} - 1) \\
& \quad + \langle \boldsymbol{\lambda}_1, \mathbf{S}^\top \mathbf{1} - \mathbf{1} \rangle + \lambda_2 (\mathbf{c}^\top \mathbf{S} \mathbf{1} + \beta - \Omega) \\
& \quad + \langle \boldsymbol{\lambda}_3, \mathbf{D} \mathbf{S} \mathbf{1} - \mathbf{q} \rangle + \langle \boldsymbol{\lambda}_4, \mathbf{A} \mathbf{S} \mathbf{1} - \boldsymbol{\gamma} \rangle \\
& \quad + \frac{\rho}{2} \|\mathbf{S}^\top \mathbf{1} - \mathbf{1}\|^2 + \frac{\rho}{2} (\mathbf{c}^\top \mathbf{S} \mathbf{1} + \beta - \Omega)^2 \\
& \quad + \frac{\rho}{2} \|\mathbf{D} \mathbf{S} \mathbf{1} - \mathbf{q}\|^2 + \frac{\rho}{2} \|\mathbf{A} \mathbf{S} \mathbf{1} - \boldsymbol{\gamma}\|^2 \\
\beta^{t+1} &= \underset{\beta}{\operatorname{argmin}} \quad \mathbb{I}_{\mathbb{R}^+}(\beta) + \lambda_2 (\mathbf{c}^\top \mathbf{S} \mathbf{1} + \beta - \Omega) + \frac{\rho}{2} (\mathbf{c}^\top \mathbf{S} \mathbf{1} + \beta - \Omega)^2 \\
\boldsymbol{\gamma}^{t+1} &= \underset{\boldsymbol{\gamma}}{\operatorname{argmin}} \quad F_{tt}(\boldsymbol{\gamma}) + \langle \boldsymbol{\lambda}_4, \mathbf{A} \mathbf{S} \mathbf{1} - \boldsymbol{\gamma} \rangle + \frac{\rho}{2} \|\mathbf{A} \mathbf{S} \mathbf{1} - \boldsymbol{\gamma}\|^2 \\
\boldsymbol{\lambda}_1^{t+1} &= \boldsymbol{\lambda}_1^t + \rho (\mathbf{S}^{t+1 \top} \mathbf{1} - \mathbf{1}) \\
\lambda_2^{t+1} &= \lambda_2^t + \rho (\mathbf{c}^\top \mathbf{S}^{t+1} \mathbf{1} + \beta^{t+1} - \Omega) \\
\boldsymbol{\lambda}_3^{t+1} &= \boldsymbol{\lambda}_3^t + \rho (\mathbf{D} \mathbf{S}^{t+1} \mathbf{1} - \mathbf{q}) \\
\boldsymbol{\lambda}_4^{t+1} &= \boldsymbol{\lambda}_4^t + \rho (\mathbf{A} \mathbf{S}^{t+1} \mathbf{1} - \boldsymbol{\gamma}^{t+1})
\end{aligned}$$

We can write the update of the primal variable  $\mathbf{S}$  as a closed-form expression. To facilitate the derivation of its updating rule, we substitute  $\mathbf{S} \mathbf{1}$  in our problem with the new variable  $\mathbf{u}$  and add the constraint  $\mathbf{S} \mathbf{1} = \mathbf{u}$  to our formulation. Moreover, we substitute the matrix  $\mathbf{S}$  by the new variable  $\mathbf{W}$  in the constraint  $\mathbf{S}^\top \mathbf{1} = \mathbf{1}$  and replace the matrix  $\mathbf{S}$  with the new variable  $\mathbf{H}$  in the constraint  $\mathbf{S} \in [0, 1]^{(|\mathcal{R}| \cdot |\mathcal{I}|) \times |\mathcal{N}|}$  and the regularizer  $\mathfrak{R}(\mathbf{S})$ . As matrices  $\mathbf{W}$  and  $\mathbf{H}$  are substitutions for  $\mathbf{S}$ , we include the constraints  $\mathbf{S} = \mathbf{W}$  and  $\mathbf{S} = \mathbf{H}$  in the reformulation. Therefore,

optimization problem (13) will be reformulated as

$$\begin{aligned}
& \min_{\boldsymbol{\gamma}, \mathbf{u}, \mathbf{S}, \mathbf{W}, \mathbf{H}, \mathbf{z}, \beta} \sum_{\ell=1}^{|\mathcal{E}|} \sum_{t=1}^{|\mathcal{T}|} \gamma_{\ell,t} \delta(\gamma_{\ell,t}) \\
& \quad - \frac{\tilde{\lambda}}{2} \sum_{r=1}^{|\mathcal{R}|} \sum_{i=1}^{|\mathcal{I}|} \sum_{n=1}^{|\mathcal{N}|} \mathbf{H}_{r,i,n} (\mathbf{H}_{r,i,n} - 1) \\
& \text{s.t. } \mathbf{S}\mathbf{1} = \mathbf{u}, \quad \mathbf{W}^T \mathbf{1} = \mathbf{1} \\
& \quad \mathbf{D}\mathbf{u} = \mathbf{q}, \quad \mathbf{A}\mathbf{u} = \boldsymbol{\gamma} \\
& \quad \mathbf{H} = \mathbf{S}, \quad \mathbf{W} = \mathbf{S} \\
& \quad \mathbf{c}^T \mathbf{u} + \beta = \Omega, \quad \beta \geq 0 \\
& \quad \mathbf{H} \in [0, 1]^{(|\mathcal{R}| \cdot |\mathcal{I}|) \times |\mathcal{N}|}.
\end{aligned} \tag{15}$$

which is the introduced problem (8) in the subsection II-C. Let

$$\begin{aligned}
& \mathcal{L}(\boldsymbol{\gamma}, \mathbf{S}, \mathbf{H}, \mathbf{W}, \mathbf{u}, \beta) \\
& \triangleq F_{tt}(\boldsymbol{\gamma}) + \mathbb{I}_{[0,1]^{(|\mathcal{R}| \cdot |\mathcal{I}|) \times |\mathcal{N}|}}(\mathbf{H}) + \mathbb{I}_{\mathbb{R}^+}(\beta) \\
& \quad + \langle \boldsymbol{\lambda}_1, \mathbf{S}\mathbf{1} - \mathbf{u} \rangle + \langle \boldsymbol{\lambda}_2, \mathbf{W}^T \mathbf{1} - \mathbf{1} \rangle + \langle \boldsymbol{\lambda}_3, \mathbf{D}\mathbf{u} - \mathbf{q} \rangle \\
& \quad + \langle \boldsymbol{\lambda}_4, \mathbf{A}\mathbf{u} - \boldsymbol{\gamma} \rangle + \langle \boldsymbol{\Lambda}_5, \mathbf{H} - \mathbf{S} \rangle \\
& \quad + \lambda_6 (\mathbf{c}^T \mathbf{u} + \beta - \Omega) + \langle \boldsymbol{\Lambda}_7, \mathbf{W} - \mathbf{S} \rangle \\
& \quad + \frac{\rho}{2} \|\mathbf{S}\mathbf{1} - \mathbf{u}\|^2 + \frac{\rho}{2} \|\mathbf{W}^T \mathbf{1} - \mathbf{1}\|^2 \\
& \quad + \frac{\rho}{2} \|\mathbf{D}\mathbf{u} - \mathbf{q}\|^2 + \frac{\rho}{2} \|\mathbf{A}\mathbf{u} - \boldsymbol{\gamma}\|^2 \\
& \quad + \frac{\rho}{2} \|\mathbf{H} - \mathbf{S}\|^2 + \frac{\rho}{2} (\mathbf{c}^T \mathbf{u} + \beta - \Omega)^2 \\
& \quad + \frac{\rho}{2} \|\mathbf{W} - \mathbf{S}\|^2 - \frac{\tilde{\lambda}}{2} \sum_{r=1}^{|\mathcal{R}|} \sum_{i=1}^{|\mathcal{I}|} \sum_{n=1}^{|\mathcal{N}|} \mathbf{H}_{r,i,n} (\mathbf{H}_{r,i,n} - 1)
\end{aligned} \tag{16}$$

be the augmented Lagrangian function of (8) with the set of Lagrange multipliers  $\{\boldsymbol{\lambda}_1, \boldsymbol{\lambda}_2, \dots, \boldsymbol{\Lambda}_7\}$  and  $\rho > 0$  be the primal penalty parameter. Then, ADMM solves (8) by the following iterative scheme

$$\begin{aligned}
\mathbf{u}^{t+1} &= \underset{\mathbf{u}}{\operatorname{argmin}} \quad \langle \boldsymbol{\lambda}_1^t, \mathbf{S}^{t+1} \mathbf{1} - \mathbf{u} \rangle + \langle \boldsymbol{\lambda}_3^t, \mathbf{D}\mathbf{u} - \mathbf{q} \rangle \\
& \quad + \langle \boldsymbol{\lambda}_4^t, \mathbf{A}\mathbf{u} - \boldsymbol{\gamma} \rangle + \lambda_6 (\mathbf{c}^T \mathbf{u} + \beta - \Omega) \\
& \quad + \frac{\rho}{2} \|\mathbf{S}^{t+1} \mathbf{1} - \mathbf{u}\|^2 + \frac{\rho}{2} \|\mathbf{D}\mathbf{u} - \mathbf{q}\|^2 \\
& \quad + \frac{\rho}{2} \|\mathbf{A}\mathbf{u} - \boldsymbol{\gamma}\|^2 + \frac{\rho}{2} (\mathbf{c}^T \mathbf{u} + \beta - \Omega)^2 \\
\mathbf{W}^{t+1} &= \underset{\mathbf{W}}{\operatorname{argmin}} \quad \langle \boldsymbol{\lambda}_2^t, \mathbf{W}^T \mathbf{1} - \mathbf{1} \rangle + \langle \boldsymbol{\Lambda}_7^t, \mathbf{W} - \mathbf{S}^{t+1} \rangle \\
& \quad + \frac{\rho}{2} \|\mathbf{W}^T \mathbf{1} - \mathbf{1}\|^2 + \frac{\rho}{2} \|\mathbf{W} - \mathbf{S}^{t+1}\|^2 \\
\mathbf{H}^{t+1} &= \underset{\mathbf{H}}{\operatorname{argmin}} \quad \mathbb{1}(\rho > \tilde{\lambda}) \mathbb{I}_{[0,1]^{(|\mathcal{R}| \cdot |\mathcal{I}|) \times |\mathcal{N}|}}(\mathbf{H}) \\
& \quad + \mathbb{1}(\rho < \tilde{\lambda}) \mathbb{I}_{\{0,1\}^{(|\mathcal{R}| \cdot |\mathcal{I}|) \times |\mathcal{N}|}}(\mathbf{H})
\end{aligned}$$

$$\begin{aligned}
& + \langle \Lambda_5^t, \mathbf{H} - \mathbf{S}^{t+1} \rangle + \frac{\rho}{2} \|\mathbf{H} - \mathbf{S}^{t+1}\|^2 \\
& - \frac{\tilde{\lambda}}{2} \sum_{r=1}^{|\mathcal{R}|} \sum_{i=1}^{|\mathcal{I}|} \sum_{n=1}^{|\mathcal{N}|} \mathbf{H}_{r,i,n} (\mathbf{H}_{r,i,n} - 1) \\
\mathbf{S}^{t+1} = \operatorname{argmin}_{\mathbf{S}} & \langle \lambda_1^t, \mathbf{S} \mathbf{1} - \mathbf{u}^t \rangle + \langle \Lambda_5^t, \mathbf{H}^t - \mathbf{S} \rangle \\
& + \langle \Lambda_7^t, \mathbf{W}^t - \mathbf{S} \rangle + \frac{\rho}{2} \|\mathbf{S} \mathbf{1} - \mathbf{u}^t\|^2 \\
& + \frac{\rho}{2} \|\mathbf{H}^t - \mathbf{S}\|^2 + \frac{\rho}{2} \|\mathbf{W}^t - \mathbf{S}\|^2 \\
\beta^{t+1} = \operatorname{argmin}_{\beta} & \mathbb{I}_+(\beta) + \lambda_6^t (\mathbf{c}^\top \mathbf{u}^{t+1} + \beta - \Omega) \\
& + \frac{\rho}{2} (\mathbf{c}^\top \mathbf{u}^{t+1} + \beta - \Omega)^2 \\
\lambda_1^{t+1} = & \lambda_1^t + \rho (\mathbf{S}^{t+1} \mathbf{1} - \mathbf{u}^{t+1}) \\
\lambda_2^{t+1} = & \lambda_2^t + \rho (\mathbf{W}^{t+1} \mathbf{1} - \mathbf{1}) \\
\lambda_3^{t+1} = & \lambda_3^t + \rho (\mathbf{D} \mathbf{u}^{t+1} - \mathbf{q}) \\
\lambda_4^{t+1} = & \lambda_4^t + \rho (\mathbf{A} \mathbf{u}^{t+1} - \gamma^{t+1}) \\
\Lambda_5^{t+1} = & \Lambda_5^t + \rho (\mathbf{H}^{t+1} - \mathbf{S}^{t+1}) \\
\lambda_6^{t+1} = & \lambda_6^t + \rho (\mathbf{c}^\top \mathbf{u}^{t+1} + \beta^{t+1} - \Omega) \\
\Lambda_7^{t+1} = & \Lambda_7^t + \rho (\mathbf{W}^{t+1} - \mathbf{S}^{t+1})
\end{aligned}$$

The primal update rules can be simplified as

$$\begin{aligned}
\gamma_{\ell, \hat{t}}^{t+1} = \operatorname{argmin}_{\gamma_{\ell, \hat{t}}} & \gamma_{\ell, \hat{t}} \delta(\gamma_{\ell, \hat{t}}) + \lambda_{4, (\ell, \hat{t})}^t (\mathbf{a}_{\ell, \hat{t}} \mathbf{u}^t - \gamma_{\ell, \hat{t}}) \\
& + \frac{\rho}{2} (\mathbf{a}_{\ell, \hat{t}} \mathbf{u}^t - \gamma_{\ell, \hat{t}})^2, \quad \forall \ell, \forall \hat{t} \\
\mathbf{S}^{t+1} = \frac{1}{\rho} & (-\lambda_1^t \mathbf{1}^\top + \Lambda_5^t + \Lambda_7^t + \rho \mathbf{u}^t \mathbf{1}^\top + \rho \mathbf{H}^t \\
& + \rho \mathbf{W}^t) (\mathbf{1} \mathbf{1}^\top + 2\mathbf{I})^{-1} \\
\mathbf{H}^{t+1} = \mathbb{I}(\rho > \tilde{\lambda}) \Pi & \left( \left( \frac{1}{\rho - \tilde{\lambda}} \right) (\rho \mathbf{S}^t - \Lambda_5^t - \frac{\tilde{\lambda}}{2}) \right)_{[0,1]} \\
& + \mathbb{I}(\rho < \tilde{\lambda}) \Pi \left( \left( \frac{1}{\rho - \tilde{\lambda}} \right) (\rho \mathbf{S}^t - \Lambda_5^t - \frac{\tilde{\lambda}}{2}) \right)_{\{0,1\}} \\
\mathbf{W}^{t+1} = \frac{1}{\rho} & (\mathbf{I} + \mathbf{1} \mathbf{1}^\top)^{-1} (-\lambda_2^t \mathbf{1}^\top - \Lambda_7^t + \rho \mathbf{1} \mathbf{1}^\top + \rho \mathbf{S}^{t+1}) \\
\mathbf{u}^{t+1} = \frac{1}{\rho} & (\mathbf{I} + \mathbf{D}^\top \mathbf{D} + \mathbf{A}^\top \mathbf{A} + \mathbf{c} \mathbf{c}^\top)^{-1} (\lambda_1^t - \mathbf{D}^\top \lambda_3^t - \mathbf{A}^\top \lambda_4^t \\
& + \rho \mathbf{S}^{t+1} \mathbf{1} + \rho \mathbf{D}^\top \mathbf{q} + \rho \mathbf{A}^\top \gamma^{t+1} - \lambda_6 \mathbf{c} - \beta \rho \mathbf{c} + \Omega \rho \mathbf{c}) \\
\beta^{t+1} = \Pi & \left( \frac{1}{\rho} (-\lambda_6^t - \rho \mathbf{c}^\top \mathbf{u}^t + \rho \Omega) \right)_{\mathbb{R}_+}
\end{aligned}$$

## APPENDIX C

## DISTRIBUTED COMPUTATION OF ALGORITHM 1

To handle the expensive computation of matrices  $\mathbf{W}$ ,  $\mathbf{H}$ , and  $\mathbf{S}$  in Algorithm 1, we can utilize the computational power of our drivers' smartphones. Each column of the matrices  $\mathbf{W}$ ,  $\mathbf{H}$ , and  $\mathbf{S}$  corresponds to a single driver, and hence the computation corresponding to each column can be performed in parallel on smartphone devices of the drivers. The details of this parallel computation are depicted in Figure 11. To update the  $i^{\text{th}}$  column of matrices  $\mathbf{W}$ ,  $\mathbf{H}$ , and  $\mathbf{S}$  at iteration  $t$  of Algorithm 1, driver  $i$ 's smartphone computes

$$\begin{aligned}\mathbf{W}_{(:,i)}^{t+1} &= (\rho \mathbf{1} \mathbf{1}^\top + \rho \mathbf{I})^{-1} (\rho \mathbf{1} + \rho \mathbf{S}_{(:,i)}^t - \mathbf{\Lambda}_{7,(:,i)}^t - \mathbf{\lambda}_{2,(:,i)}^t) \\ \mathbf{H}_{(:,i)}^{t+1} &= \mathbb{1}(\rho > \tilde{\lambda}) \Pi \left( \left( \frac{1}{\rho - \tilde{\lambda}} \right) (\rho \mathbf{S}_{(:,i)}^t - \mathbf{\Lambda}_{5,(:,i)}^t - \frac{\tilde{\lambda}}{2}) \right)_{[0,1]} \\ &\quad + \mathbb{1}(\rho < \tilde{\lambda}) \Pi \left( \left( \frac{1}{\rho - \tilde{\lambda}} \right) (\rho \mathbf{S}_{(:,i)}^t - \mathbf{\Lambda}_{5,(:,i)}^t - \frac{\tilde{\lambda}}{2}) \right)_{\{0,1\}} \\ \mathbf{S}_{(:,i)}^{t+1} &= (\rho \mathbf{u}^{t+1} \mathbf{1}^\top + \mathbf{\Lambda}_{5,(:,i)}^t + \rho \mathbf{H}_{(:,i)}^{t+1} + \mathbf{\Lambda}_{7,(:,i)}^t + \rho \mathbf{W}_{(:,i)}^{t+1} - \mathbf{\lambda}_1^t \mathbf{1}^\top) (\rho \mathbf{1} \mathbf{1}^\top + 2\rho \mathbf{I})^{-1}\end{aligned}$$

where  $(:, i)$  denotes the  $i^{\text{th}}$  column of the matrix and corresponds to the driver  $i$ .

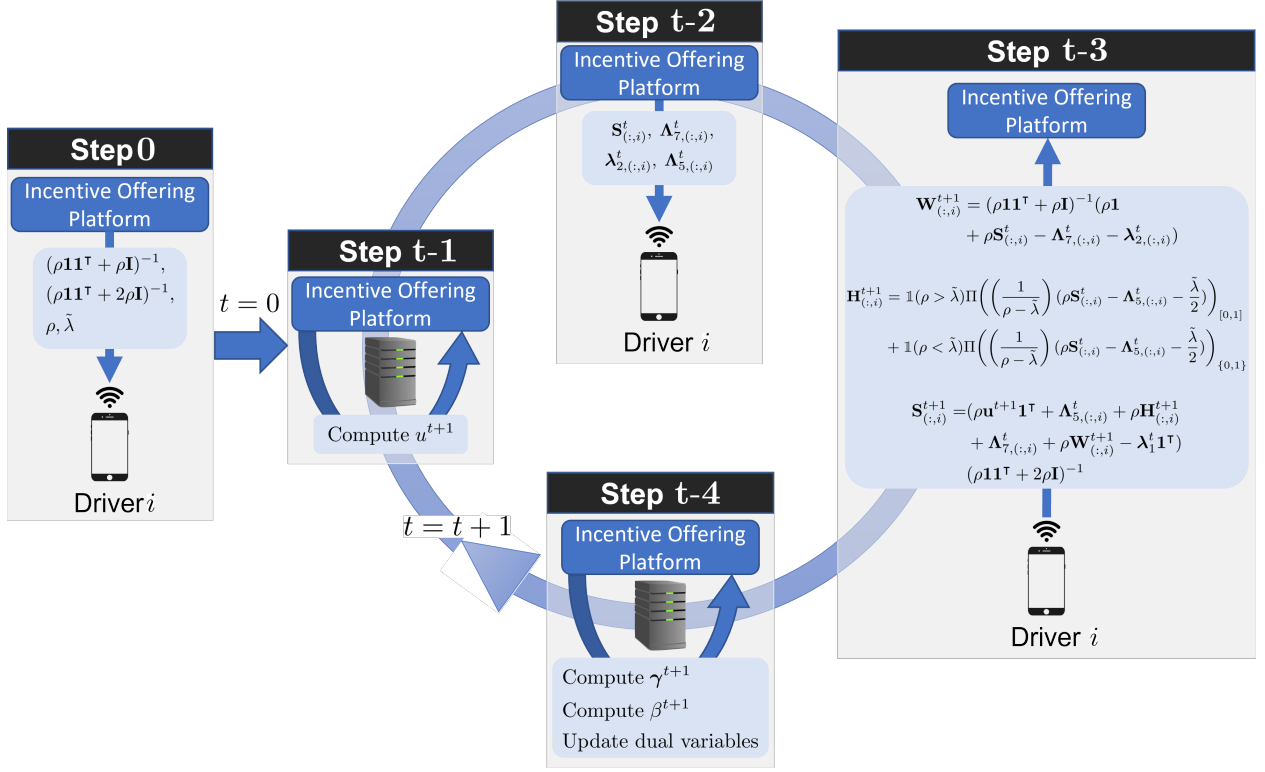


Fig. 11. Steps of distributed implementation of Algorithm 1. Step 0: Incentive offering platform shares the constant parameters and matrices with drivers. Step t-1: The incentive offering platform updates  $\mathbf{u}^{t+1}$ . Step t-2: Incentive offering platform sends the required information to drivers. Step t-3: Incentive offering platform receives the updated vectors from drivers. Step t-4: Incentive offering platform updates  $\gamma^{t+1}$ ,  $\beta^{t+1}$ , and dual variables.

## APPENDIX D

### UE ALGORITHM

In our numerical experiments, we use the volume at the UE state of the system after the incentivization to evaluate the travel time. To compute the volume at User Equilibrium, we present Algorithm 2. Before we present the details of Algorithm 2, let us explain some notations used in this algorithm. Vector  $\mathbf{v} \in \mathbb{R}_+^{|\mathcal{E}| \cdot |\mathcal{T}|}$  denotes the volume of links at different time slots.  $\mathcal{N}_1$  is the set of user drivers that accept the incentive offer and  $\mathbf{S}_1 \in \{0, 1\}^{|\mathcal{R}| \times |\mathcal{N}_1|}$  is the matrix of route assignment of these drivers.  $\mathcal{N}_2$  is the set of the remaining drivers (user drivers that rejected the incentive offer, user drivers that did not receive an incentive offer, and nonuser drivers) and  $\mathbf{S}_2 \in \{0, 1\}^{|\mathcal{E}| \times |\mathcal{N}_2|}$  is the matrix of their OD assignment.  $\tilde{\mathbf{P}} \in [0, 1]^{|\mathcal{R}| \times |\mathcal{E}|}$  encodes the information of probability of picking different routes given the driver's OD. Thus, the vector  $\tilde{\mathbf{P}} \mathbf{S}_2 \mathbf{1} \in \mathbb{R}^{|\mathcal{R}| \times 1}$  shows the expected number of non-incentivized vehicles in each route.  $\delta_{\text{UE}} \in \mathbb{R}_+$  is the total travel time of the system based on the traffic volume at the last iteration.

---

**Algorithm 2** Computation of Travel Time at UE
 

---

- 1: **Input:** Step size:  $\alpha_{\text{UE}}$ , Number of iterations:  $\tilde{T}$ .
  - 2: Compute  $\mathbf{R}_0$  and  $\tilde{\mathbf{P}}_0$  using volume vector  $\mathbf{v}_0$  (historical data)
  - 3: **for**  $t = 1, 2, \dots, \tilde{T}$  **do**
  - 4:    $\tilde{\mathbf{v}}_t = \mathbf{R}_{t-1}\mathbf{S}_1\mathbf{1} + \mathbf{R}_{t-1}\tilde{\mathbf{P}}_{t-1}\mathbf{S}_2\mathbf{1}$
  - 5:    $\mathbf{v}_t = (1 - \alpha_{\text{UE}})\mathbf{v}_{t-1} + \alpha_{\text{UE}}\tilde{\mathbf{v}}_t$
  - 6:   Compute  $\mathbf{R}_t$  and  $\tilde{\mathbf{P}}_t$  based on volume vector  $\mathbf{v}_t$
  - 7: **end for**
  - 8: Compute UE travel time  $\delta_{\text{UE}}$  utilizing  $\mathbf{v}_{\tilde{T}}$  and BPR function
  - 9: **Return:**  $\delta_{\text{UE}}$
- 

In this algorithm, we rely on the method presented by [57] to compute matrix  $\mathbf{R}$  and  $\tilde{\mathbf{P}}$  based on the volume vector  $\mathbf{v}$ .

## APPENDIX E

## AN EXAMPLE OF THE MODEL AND NOTATIONS

In this section, we present a small example of a network to illustrate our model and notations. Consider the network



Fig. 12. Network example  $\mathcal{G}_1$ .

where  $\mathcal{V} = \{\nu_1, \nu_2, \nu_3\}$  is the set of nodes and  $\mathcal{E} = \{e_1, e_2, e_3\}$  is the set edges (roads). Details of the links and attributes are represented in TABLE VIII. The (origin, destination) pair is  $(\nu_1, \nu_3)$ . There are two routes going from origin to destination as illustrated in TABLE IX. The time horizon set is  $\mathbf{T} = \{1, 2, 3\}$  and each time is 0.2 hour. To estimate the location of drivers at each time, we need matrix  $\mathbf{R} \in [0, 1]^{9 \times 6}$  as follows

$$\mathbf{R} = \begin{array}{c}
 \begin{array}{cccccc}
 & t_1 & t_1 & t_1 & t_1 & t_1 & t_1 \\
 = & 1 & = 1 & = 2 & = 2 & = 3 & = 3 \\
 \mathbf{r}_1 & \mathbf{r}_2 & \mathbf{r}_1 & \mathbf{r}_2 & \mathbf{r}_1 & \mathbf{r}_2 & \\
 \begin{array}{l}
 t_2 = 1, e_1 \\
 t_2 = 1, e_2 \\
 t_2 = 1, e_3 \\
 t_2 = 2, e_1 \\
 t_2 = 2, e_2 \\
 t_2 = 2, e_3 \\
 t_2 = 3, e_1 \\
 t_2 = 3, e_2 \\
 t_2 = 3, e_3
 \end{array}
 & \left( \begin{array}{cccccc}
 1 & 1 & 0 & 0 & 0 & 0 \\
 0 & 0 & 0 & 0 & 0 & 0 \\
 0.5 & 0 & 0 & 0 & 0 & 0 \\
 0 & 0 & 1 & 1 & 0 & 0 \\
 0 & 1 & 0 & 0 & 0 & 0 \\
 0.5 & 0 & 0.5 & 0 & 0 & 0 \\
 0 & 0 & 0 & 0 & 1 & 1 \\
 0 & 0 & 0 & 1 & 0 & 0 \\
 0 & 0 & 0.5 & 0 & 0.5 & 0
 \end{array} \right)
 \end{array}
 \end{array}$$

	Length (Mile)	Speed (mph)	Travel time (Hour)
$e_1$	5	50	0.1
$e_2$	10	50	0.2
$e_3$	5	50	0.1

TABLE VIII  
SET OF EDGES.

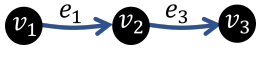
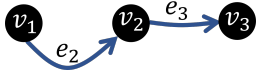
	$\mathbf{r}$	Graph
Route 1 $e_1 \rightarrow e_3$	$\mathbf{r}_1 = \begin{bmatrix} 1 \\ 0 \\ 1 \end{bmatrix}$	
Route 2 $e_2 \rightarrow e_3$	$\mathbf{r}_2 = \begin{bmatrix} 0 \\ 1 \\ 1 \end{bmatrix}$	

TABLE IX  
SET OF ROUTES.

where  $t_1$  is the entrance time of the driver and  $t_2$  is the driver's arrival time at the road. In model (3), the column vector  $\beta_{\mathbf{r},t}$  corresponds to the columns of matrix  $\mathbf{R}$ .

Assume there are two drivers in the system and  $\mathcal{N} = \{d_1, d_2\}$ . We want to offer rewards from the set  $\mathcal{I} = \{\$0, \$5\}$  to control the traffic. To estimate the probability of choosing routes given an offered incentive at a time, we use matrix  $\mathbf{P} \in [0, 1]^{6 \times 12}$  when incentive  $i$  is offered:

$$\mathbf{P}_{t_i} = \begin{matrix} & \text{No incentive} & \$5 \rightarrow \mathbf{r}_1 & \$5 \rightarrow \mathbf{r}_2 \\ \begin{matrix} t = 1, \mathbf{r}_1 \\ t = 1, \mathbf{r}_2 \\ t = 2, \mathbf{r}_1 \\ t = 2, \mathbf{r}_2 \\ t = 3, \mathbf{r}_1 \\ t = 3, \mathbf{r}_2 \end{matrix} & \begin{pmatrix} 0.50 & 0.50 & 0.97 & 0.03 \\ 0.50 & 0.50 & 0.03 & 0.97 \\ 0.50 & 0.50 & 0.97 & 0.03 \\ 0.50 & 0.50 & 0.03 & 0.97 \\ 0.50 & 0.50 & 0.97 & 0.03 \\ 0.50 & 0.50 & 0.03 & 0.97 \end{pmatrix} \end{matrix}$$

$, \forall i \in \{1, 2, 3\}$

$$\mathbf{P} = \begin{bmatrix} \mathbf{P}_{t_1} & \mathbf{P}_{t_2} & \mathbf{P}_{t_3} \end{bmatrix}$$

Probability matrices for all three times are equal because the speed is the same in all three times. We compute the probability of choosing route  $k$  given that  $\$i'$  is offered for route  $j'$  by

$$\begin{aligned} & \mathbb{P}(\mathbf{r} = k, i = (\$i' \rightarrow \text{route } j')) \\ &= \frac{\exp(-0.086tt_k + 0.7i'\mathbb{I}_{k=j'})}{\exp(-0.086tt_{j'} + 0.7i') + \sum_{j \neq j'} \exp(-0.086tt_j)} \end{aligned} \quad (17)$$

where  $tt_j$  is the travel time of route  $j$ . We use [55] to extract these coefficients.

APPENDIX F  
DETAILS OF THE NUMERICAL EXPERIMENTS

		Budget	Incentive		
			\$0	\$2	\$10
Penetration Rate	25%	\$1000	7242	191	61
		\$10000	7198	14	282
	50%	\$1000	7063	414	17
		\$10000	6975	0	519
	75%	\$1000	6994	500	0
		\$10000	6717	0	777
	100%	\$1000	6994	500	0
		\$10000	6472	28	994

TABLE X

DISTRIBUTION OF THE OFFERED INCENTIVES IN EXPERIMENT I WITH DIFFERENT PENETRATION RATES.

Budget	Incentive		
	\$0	\$2	\$10
\$1000	14645	435	13
\$10000	12614	1849	630

TABLE XI

DISTRIBUTION OF THE OFFERED INCENTIVES IN EXPERIMENT II FOR INCENTIVE SET  $\mathcal{I}_1$  WITH PENETRATION RATE OF 100%.

Budget	Incentive					
	\$0	\$1	\$2	\$3	\$5	\$10
\$1000	14509	351	152	30	51	0
\$10000	12682	184	305	832	838	252

TABLE XII

DISTRIBUTION OF THE OFFERED INCENTIVES IN EXPERIMENT II FOR INCENTIVE SET  $\mathcal{I}_2$  WITH PENETRATION RATE OF 100%.

Budget	Incentive		
	\$0	\$2	\$10
\$1000	7720	500	0
\$10000	6916	380	924

TABLE XIII

DISTRIBUTION OF THE OFFERED INCENTIVES IN EXPERIMENT III FOR MODEL (3) WITH PENETRATION RATE OF 100%.

		Budget	Incentive		
			\$0	\$2	\$10
Penetration Rate	25%	\$1000	8042	100	78
		\$10000	7879	104	237
	50%	\$1000	7892	285	43
		\$10000	7144	109	967
	75%	\$1000	7772	435	13
		\$10000	7057	241	922
	100%	\$1000	7720	500	0
		\$10000	7031	289	900

TABLE XIV

DISTRIBUTION OF THE OFFERED INCENTIVES IN EXPERIMENT III WITH DIFFERENT PENETRATION RATES FOR MODEL (6), ALGORITHM 1.

		Budget	Incentive		
			\$0	\$2	\$10
Penetration Rate	25%	\$1000	8032	110	78
		\$10000	7891	9	320
	50%	\$1000	7980	175	65
		\$10000	7565	0	655
	75%	\$1000	7972	185	63
		\$10000	7246	78	896
	100%	\$1000	7896	280	44
		\$10000	7022	248	950

TABLE XV

DISTRIBUTION OF THE OFFERED INCENTIVES IN EXPERIMENT III WITH DIFFERENT PENETRATION RATES FOR MODEL (6), GUROBI.

		Budget	Incentive		
			\$0	\$2	\$10
Penetration Rate	25%	\$1000	8036	105	79
		\$10000	7658	0	562
	50%	\$1000	8050	85	85
		\$10000	7220	0	1000
	75%	\$1000	7972	185	63
		\$10000	7240	83	897
	100%	\$1000	7900	286	34
		\$10000	7048	260	912

TABLE XVI

DISTRIBUTION OF THE OFFERED INCENTIVES IN EXPERIMENT III WITH DIFFERENT PENETRATION RATES FOR MODEL (6), MOSEK.

Budget	Penetration Rate			
	25%	50%	75%	100%
\$100	3	4	4	5
\$1000	11	21	27	27
\$10000	14	27	38	47

TABLE XVII

EFFECT OF THE PENETRATION RATE ON TRAVEL TIME DECREASE (HOUR) IN EXPERIMENT I.

Budget	Penetration Rate			
	25%	50%	75%	100%
\$100	0.49%	0.63%	0.62%	0.68%
\$1000	1.68%	3.07%	3.91%	4.03%
\$10000	2.03%	3.99%	5.52%	6.97%

TABLE XVIII

EFFECT OF THE PENETRATION RATE ON THE PERCENTAGE OF TRAVEL TIME DECREASE IN EXPERIMENT I.

Budget	Penetration Rate			
	25%	50%	75%	100%
\$100	8	8	4	8
\$1000	25	44	50	57
\$10000	27	50	72	96

TABLE XIX

EFFECT OF THE PENETRATION RATE ON TRAVEL TIME DECREASE (HOUR) IN EXPERIMENT III, MODEL (6), ALGORITHM 1.

Budget	Penetration Rate			
	25%	50%	75%	100%
\$100	0.38%	0.41%	0.17%	0.37%
\$1000	1.21%	2.13%	2.41%	2.71%
\$10000	1.28%	2.38%	3.47%	4.60%

TABLE XX

EFFECT OF THE PENETRATION RATE ON THE PERCENTAGE OF TRAVEL TIME DECREASE IN EXPERIMENT III, MODEL (6), ALGORITHM 1.

Budget	Penetration Rate			
	25%	50%	75%	100%
\$100	8	9	7	6
\$1000	23	43	49	65
\$10000	28	55	74	98

TABLE XXI

EFFECT OF THE PENETRATION RATE ON TRAVEL TIME DECREASE (HOUR) IN EXPERIMENT III, MODEL (6), GUROBI.

Budget	Penetration Rate			
	25%	50%	75%	100%
\$100	0.38%	0.45%	0.33%	0.30%
\$1000	1.10%	2.06%	2.33%	3.09%
\$10000	1.32%	2.64%	3.56%	4.69%

TABLE XXII

EFFECT OF THE PENETRATION RATE ON THE PERCENTAGE OF TRAVEL TIME DECREASE IN EXPERIMENT III, MODEL (6), GUROBI.

Budget	Penetration Rate			
	25%	50%	75%	100%
\$100	8	8	5	6
\$1000	23	29	48	67
\$10000	28	62	70	101

TABLE XXIII

EFFECT OF THE PENETRATION RATE ON TRAVEL TIME DECREASE (HOUR) IN EXPERIMENT III, MODEL (6), MOSEK.

Budget	Penetration Rate			
	25%	50%	75%	100%
\$100	0.38%	0.37%	0.23%	0.27%
\$1000	1.11%	1.39%	2.31%	3.19%
\$10000	1.33%	2.98%	3.35%	4.86%

TABLE XXIV

EFFECT OF THE PENETRATION RATE ON THE PERCENTAGE OF TRAVEL TIME DECREASE IN EXPERIMENT III, MODEL (6), MOSEK.

## REFERENCES

- [1] "INRIX 2019 Global Traffic Scorecard," <https://inrix.com/scorecard/>, Accessed: 2023-02-15.
- [2] National Research Council (US). Committee for the Evaluation of the Congestion Mitigation and Air Quality Improvement Program and National Research Council, The congestion mitigation and air quality improvement program: assessing 10 years of experience. Transportation Research Board, 2002, vol. 264.
- [3] Health Effects Institute. Panel on the Health Effects of Traffic-Related Air Pollution, Traffic-related air pollution: a critical review of the literature on emissions, exposure, and health effects. Health Effects Institute, 2010, no. 17.
- [4] K. Zhang and S. Batterman, "Air pollution and health risks due to vehicle traffic," Science of the total Environment, vol. 450, pp. 307–316, 2013.
- [5] D. A. Hennessy and D. L. Wiesenthal, "Traffic congestion, driver stress, and driver aggression," Aggressive Behavior: Official Journal of the International Society for Research on Aggression, vol. 25, no. 6, pp. 409–423, 1999.

- [6] M. L. Selzer and A. Vinokur, "Life events, subjective stress, and traffic accidents," American Journal of Psychiatry, vol. 131, no. 8, pp. 903–906, 1974.
- [7] A. C. Pigou, "The economics of welfare Macmillan and Co," London, United Kingdom, 1920.
- [8] F. H. Knight, "Some fallacies in the interpretation of social cost," The Quarterly Journal of Economics, vol. 38, no. 4, pp. 582–606, 1924.
- [9] E. Verhoef, M. C. Bliemer, L. Steg, and B. van Wee, Eds., Pricing in Road Transport, ser. Books. Edward Elgar Publishing, July 2008, no. 4192. [Online]. Available: <https://ideas.repec.org/b/elg/eebook/4192.html>
- [10] D. H. Van Amelsfort, "Behavioural responses and network effects of time-varying road pricing," 2009.
- [11] S. Bouchelaghem and M. Omar, "Reliable and secure distributed smart road pricing system for smart cities," IEEE Transactions on Intelligent Transportation Systems, vol. 20, no. 5, pp. 1592–1603, 2018.
- [12] N. Zheng, G. R erat, and N. Geroliminis, "Time-dependent area-based pricing for multimodal systems with heterogeneous users in an agent-based environment," Transportation Research Part C: Emerging Technologies, vol. 62, pp. 133–148, 2016.
- [13] C. F. Daganzo and L. J. Lehe, "Distance-dependent congestion pricing for downtown zones," Transportation Research Part B: Methodological, vol. 75, pp. 89–99, 2015.
- [14] S. Zhang, A. M. Campbell, and J. F. Ehmke, "Impact of congestion pricing schemes on costs and emissions of commercial fleets in urban areas," Networks, vol. 73, no. 4, pp. 466–489, 2019.
- [15] J. Knockaert, Y.-Y. Tseng, E. T. Verhoef, and J. Rouwendal, "The Spitsmijden experiment: A reward to battle congestion," Transport Policy, vol. 24, pp. 260–272, 2012.
- [16] D. Levinson, "Equity effects of road pricing: A review," Transport Reviews, vol. 30, no. 1, pp. 33–57, 2010.
- [17] K. Martens, A. Golub, and G. Robinson, "A justice-theoretic approach to the distribution of transportation benefits: Implications for transportation planning practice in the United States," Transportation Research Part A: Policy and Practice, vol. 46, no. 4, pp. 684–695, 2012.
- [18] C. Raux and S. Souche, "The acceptability of urban road pricing: A theoretical analysis applied to experience in Lyon," Journal of Transport Economics and Policy (JTEP), vol. 38, no. 2, pp. 191–215, 2004.
- [19] P. Ieromonachou, S. Potter, and J. P. Warren, "Evaluation of the implementation process of urban road pricing schemes in the United Kingdom and Italy," European Transport, vol. 32, pp. 49–68, 2006.
- [20] D. A. Hensher and M. C. Bliemer, "What type of road pricing scheme might appeal to politicians? viewpoints on the challenge in gaining the citizen and public servant vote by staging reform," Transportation Research Part A: Policy and Practice, vol. 61, pp. 227–237, 2014.
- [21] Z. Gu, Z. Liu, Q. Cheng, and M. Saberi, "Congestion pricing practices and public acceptance: A review of evidence," Case Studies on Transport Policy, vol. 6, no. 1, pp. 94–101, 2018.
- [22] E. Verhoef, P. Nijkamp, and P. Rietveld, "Tradeable permits: their potential in the regulation of road transport externalities," Environment and Planning B: Planning and Design, vol. 24, no. 4, pp. 527–548, 1997.

- [23] J. M. Viegas, "Making urban road pricing acceptable and effective: searching for quality and equity in urban mobility," Transport Policy, vol. 8, no. 4, pp. 289–294, 2001.
- [24] C. Raux, "The use of transferable permits in transport policy," Transportation Research Part D: Transport and Environment, vol. 9, no. 3, pp. 185–197, 2004.
- [25] W. Fan and X. Jiang, "Tradable mobility permits in roadway capacity allocation: Review and appraisal," Transport Policy, vol. 30, pp. 132–142, 2013.
- [26] J. Thøgersen and B. Møller, "Breaking car use habits: The effectiveness of a free one-month travelcard," Transportation, vol. 35, no. 3, pp. 329–345, 2008.
- [27] G. Wang, Z. Gao, M. Xu, and H. Sun, "Models and a relaxation algorithm for continuous network design problem with a tradable credit scheme and equity constraints," Computers & Operations Research, vol. 41, pp. 252–261, 2014.
- [28] T. Tsekeris and S. Voß, "Design and evaluation of road pricing: state-of-the-art and methodological advances," NETNOMICS: Economic Research and Electronic Networking, vol. 10, no. 1, pp. 5–52, 2009.
- [29] Y. M. Nie, "A new tradable credit scheme for the morning commute problem," Networks and Spatial Economics, vol. 15, no. 3, pp. 719–741, 2015.
- [30] D. Wu, Y. Yin, S. Lawphongpanich, and H. Yang, "Design of more equitable congestion pricing and tradable credit schemes for multimodal transportation networks," Transportation Research Part B: Methodological, vol. 46, no. 9, pp. 1273–1287, 2012.
- [31] S. Grant-Muller and M. Xu, "The role of tradable credit schemes in road traffic congestion management," Transport Reviews, vol. 34, no. 2, pp. 128–149, 2014.
- [32] H. Fukui, "An empirical analysis of airport slot trading in the United States," Transportation Research Part B: Methodological, vol. 44, no. 3, pp. 330–357, 2010.
- [33] N. Dogterom, D. Ettema, and M. Dijst, "Tradable credits for managing car travel: a review of empirical research and relevant behavioural approaches," Transport Reviews, vol. 37, no. 3, pp. 322–343, 2017.
- [34] C. L. Azevedo, R. Seshadri, S. Gao, B. Atasoy, A. P. Akkinepally, E. Christofa, F. Zhao, J. Trancik, and M. Ben-Akiva, "Tripod: sustainable travel incentives with prediction, optimization, and personalization," in Transportation Research Board 97th Annual Meeting, 2018.
- [35] J. W. Brehm, A Theory of Psychological Reactance. New York: Academic Press, 1966.
- [36] J. Knockaert, M. Bliemer, D. Ettema, D. Joksimovic, A. Mulder, J. Rouwendal, and D. Van Amelsfort, "Experimental design and modelling Spitsmijden," Utrecht, Consortium Spitsmijden, 2007.
- [37] D. M. Kreps, "Intrinsic motivation and extrinsic incentives," The American Economic Review, vol. 87, no. 2, pp. 359–364, 1997.
- [38] K. C. Berridge, "Reward learning: reinforcement, incentives, and expectations." 2001.
- [39] D. Merugu, B. S. Prabhakar, and N. Rama, "An incentive mechanism for decongesting the roads: A pilot

- program in Bangalore,” in Proc. of ACM NetEcon Workshop. Citeseer, 2009.
- [40] J. S. Yue, C. V. Mandayam, D. Merugu, H. K. Abadi, and B. Prabhakar, “Reducing road congestion through incentives: a case study,” 2015.
- [41] M. Bliemer, M. Dicke-Ogenia, and D. Ettema, “Rewarding for avoiding the peak period: A synthesis of three studies in the Netherlands,” in European Transport Conference 2009. Citeseer, 2009.
- [42] E. Ben-Elia, D. Ettema, and H. Boeije, “Behaviour change dynamics in response to rewarding rush-hour avoidance: A qualitative research approach,” 2011.
- [43] E. Ben-Elia and D. Ettema, “Changing commuters’ behavior using rewards: A study of rush-hour avoidance,” Transportation Research Part F: Traffic Psychology and Behaviour, vol. 14, no. 5, pp. 354–368, 2011.
- [44] —, “Rewarding rush-hour avoidance: A study of commuters’ travel behavior,” Transportation Research Part A: Policy and Practice, vol. 45, no. 7, pp. 567–582, 2011.
- [45] V. Kumar, C. R. Bhat, R. M. Pendyala, D. You, E. Ben-Elia, and D. Ettema, “Impacts of incentive-based intervention on peak period traffic: experience from the Netherlands,” Transportation Research Record, vol. 2543, no. 1, pp. 166–175, 2016.
- [46] A.-A. Papadopoulos, I. Kordonis, M. Dessouky, and P. Ioannou, “Coordinated freight routing with individual incentives for participation,” IEEE Transactions on Intelligent Transportation Systems, vol. 20, no. 9, pp. 3397–3408, 2018.
- [47] I. Kordonis, M. M. Dessouky, and P. A. Ioannou, “Mechanisms for cooperative freight routing: incentivizing individual participation,” IEEE Transactions on Intelligent Transportation Systems, vol. 21, no. 5, pp. 2155–2166, 2019.
- [48] A.-A. Papadopoulos, I. Kordonis, M. M. Dessouky, and P. A. Ioannou, “Personalized pareto-improving pricing-and-routing schemes for near-optimum freight routing: An alternative approach to congestion pricing,” Transportation Research Part C: Emerging Technologies, vol. 125, p. 103004, 2021.
- [49] S. Fuji and R. Kitamura, “What does a one-month free bus ticket do to habitual drivers,” Transportation, vol. 30, pp. 81–95, 2003.
- [50] S. Bamberg, I. Ajzen, and P. Schmidt, “Choice of travel mode in the theory of planned behavior: The roles of past behavior, habit, and reasoned action,” Basic and Applied Social Psychology, vol. 25, no. 3, pp. 175–187, 2003.
- [51] G. Currie, “Free fare incentives to shift rail demand peaks—medium-term impacts,” Tech. Rep., 2011.
- [52] Z. Zhang, H. Fujii, and S. Managi, “How does commuting behavior change due to incentives? an empirical study of the Beijing Subway System,” Transportation Research Part F: Traffic Psychology and Behaviour, vol. 24, pp. 17–26, 2014.
- [53] S. Mohan, M. Klenk, and V. Bellotti, “Exploring how to personalize travel mode recommendations for urban transportation.” in IUI Workshops, 2019.

- [54] X. Zhu, F. Wang, C. Chen, and D. D. Reed, “Personalized incentives for promoting sustainable travel behaviors,” Transportation Research Part C: Emerging Technologies, 2019.
- [55] C. Xiong, M. Shahabi, J. Zhao, Y. Yin, X. Zhou, and L. Zhang, “An integrated and personalized traveler information and incentive scheme for energy efficient mobility systems,” Transportation Research Part C: Emerging Technologies, 2019.
- [56] Y. Zheng, B. Tang, W. Ding, and H. Zhou, “A neural autoregressive approach to collaborative filtering,” in International Conference on Machine Learning. PMLR, 2016, pp. 764–773.
- [57] W. Ma and Z. S. Qian, “Estimating multi-year 24/7 origin-destination demand using high-granular multi-source traffic data,” Transportation Research Part C: Emerging Technologies, vol. 96, pp. 96–121, 2018.
- [58] United States. Bureau of Public Roads, Traffic assignment manual for application with a large, high speed computer. US Department of Commerce, Bureau of Public Roads, Office of Planning, Urban Planning Division, 1964, vol. 37.
- [59] J. Perdomo, T. Zrnic, C. Mendler-Dünner, and M. Hardt, “Performative prediction,” in International Conference on Machine Learning. PMLR, 2020, pp. 7599–7609.
- [60] M. Grant and S. Boyd, “CVX: Matlab software for disciplined convex programming, version 2.1,” <http://cvxr.com/cvx>, Mar. 2014.
- [61] —, “Graph implementations for nonsmooth convex programs,” in Recent Advances in Learning and Control, ser. Lecture Notes in Control and Information Sciences, V. Blondel, S. Boyd, and H. Kimura, Eds. Springer-Verlag Limited, 2008, pp. 95–110, [http://stanford.edu/~boyd/graph\\_dcp.html](http://stanford.edu/~boyd/graph_dcp.html).
- [62] S. Boyd, N. Parikh, and E. Chu, Distributed optimization and statistical learning via the alternating direction method of multipliers. Now Publishers Inc, 2011.
- [63] D. Gabay and B. Mercier, “A dual algorithm for the solution of nonlinear variational problems via finite element approximation,” Computers & Mathematics with Applications, vol. 2, no. 1, pp. 17–40, 1976.
- [64] R. Glowinski and A. Marroco, “Sur l’approximation, par éléments finis d’ordre un, et la résolution, par pénalisation-dualité d’une classe de problèmes de dirichlet non linéaires,” ESAIM: Mathematical Modelling and Numerical Analysis-Modélisation Mathématique et Analyse Numérique, vol. 9, no. R2, pp. 41–76, 1975.
- [65] M. Hong, Z.-Q. Luo, and M. Razaviyayn, “Convergence analysis of alternating direction method of multipliers for a family of nonconvex problems,” SIAM Journal on Optimization, vol. 26, no. 1, pp. 337–364, 2016.
- [66] T. Huang, P. Singhanian, M. Sanjabi, P. Mitra, and M. Razaviyayn, “Alternating direction method of multipliers for quantization,” in International Conference on Artificial Intelligence and Statistics. PMLR, 2021, pp. 208–216.
- [67] B. Barazandeh, A. Ghafelebashi, M. Razaviyayn, and R. Sriharsha, “Efficient algorithms for estimating the parameters of mixed linear regression models,” arXiv preprint arXiv:2105.05953, 2021.
- [68] T. Li, A. K. Sahu, A. Talwalkar, and V. Smith, “Federated learning: Challenges, methods, and future directions,” IEEE Signal Processing Magazine, vol. 37, no. 3, pp. 50–60, 2020.

- [69] A. Lowy, A. Ghafelebashi, and M. Razaviyayn, “Private non-convex federated learning without a trusted server,” in International Conference on Artificial Intelligence and Statistics. PMLR, 2023.
- [70] C. Dwork, “Differential privacy,” in International Colloquium on Automata, Languages, and Programming. Springer, 2006, pp. 1–12.
- [71] B. McMahan, E. Moore, D. Ramage, S. Hampson, and B. A. y Arcas, “Communication-efficient learning of deep networks from decentralized data,” in Artificial intelligence and statistics. PMLR, 2017, pp. 1273–1282.
- [72] B. Jayaraman, L. Wang, D. Evans, and Q. Gu, “Distributed learning without distress: Privacy-preserving empirical risk minimization,” Advances in Neural Information Processing Systems, vol. 31, 2018.
- [73] M. Noble, A. Bellet, and A. Dieuleveut, “Differentially private federated learning on heterogeneous data,” in International Conference on Artificial Intelligence and Statistics. PMLR, 2022, pp. 10 110–10 145.
- [74] B. He and X. Yuan, “On the  $O(1/n)$  convergence rate of the Douglas–Rachford alternating direction method,” SIAM Journal on Numerical Analysis, vol. 50, no. 2, pp. 700–709, 2012.
- [75] H. J. Van Zuylen and L. G. Willumsen, “The most likely trip matrix estimated from traffic counts,” Transportation Research Part B: Methodological, vol. 14, no. 3, pp. 281–293, 1980.
- [76] E. Cascetta, “Estimation of trip matrices from traffic counts and survey data: a generalized least squares estimator,” Transportation Research Part B: Methodological, vol. 18, no. 4-5, pp. 289–299, 1984.
- [77] M. G. Bell, “The real time estimation of origin-destination flows in the presence of platoon dispersion,” Transportation Research Part B: Methodological, vol. 25, no. 2-3, pp. 115–125, 1991.
- [78] S. Bera and K. Rao, “Estimation of origin-destination matrix from traffic counts: the state of the art,” European Transport\Trasporti Europei, 2011.
- [79] P. Krishnakumari, H. van Lint, T. Djukic, and O. Cats, “A data driven method for OD matrix estimation,” Transportation Research Part C: Emerging Technologies, 2019.
- [80] S. Carrese, E. Cipriani, L. Mannini, and M. Nigro, “Dynamic demand estimation and prediction for traffic urban networks adopting new data sources,” Transportation Research Part C: Emerging Technologies, vol. 81, pp. 83–98, 2017.
- [81] M. Nigro, E. Cipriani, and A. del Giudice, “Exploiting floating car data for time-dependent origin–destination matrices estimation,” Journal of Intelligent Transportation Systems, vol. 22, no. 2, pp. 159–174, 2018.
- [82] J. Kim, F. Kurauchi, N. Uno, T. Hagihara, and T. Daito, “Using electronic toll collection data to understand traffic demand,” Journal of Intelligent Transportation Systems, vol. 18, no. 2, pp. 190–203, 2014.
- [83] J. C. Castillo, “Who benefits from surge pricing?” Available at SSRN 3245533, 2020.
- [84] “Github codes,” <https://github.com/ghafeleb/Congestion-Reduction-via-Personalized-Incentives>, accessed: 2023-02-15.